UNIVERSITÀ
DEGLI STUDI
DI PADOVA

DIPARTIMENTO
DI INGEGNERIA
DELL'INFORMAZIONE

DIPARTIMENTO DI INGEGNERIA DELL'INFORMAZIONE

CORSO DI LAUREA MAGISTRALE IN BIOINGEGNERIA

DESIGN AND CHARACTERIZATION OF HYDROGELS OF GELATIN AND ELASTIN FOR HEPATIC CELL CULTURE

Relatore: Prof.ssa ELISA CIMETTA

Laureando/a: LUCA PISANI

Correlatore: Prof.ssa GLORIA GALLEGO FERRER

ANNO ACCADEMICO 2021 – 2022

Data di laurea 05/10/2022

Luca Pisani: *Master Thesis,* Design and characterization of hydrogels of gelatin and elastin for hepatic cell culture, © June 2022

SUPERVISORS:
Gloria Gallego Ferrer
Raquel Naranjo Alcázar
Elisa Cimetta
LOCATION: Valencia

TIME FRAME: June 2022

"Somewhere, something incredible
is waiting to be known."

— Carl Sagan

Dedicated to my grandfather Bruno and my grandmother Lea

ABSTRACT

This work aims to demonstrate the potential of using a novel Gelatin-Elastin (GEL-ELR) hydrogel as a matrix for liver cell culture, with prospective applications for drug toxicity testing.

Gelatin (GEL), through its RGD domains, promotes cell attachment, while Elastin-Like Recombinamers (ELR) provide mechanical stiffness. Furthermore, the specific ELR used in this study contains heparin-binding sites with affinity to growth factors, to attract the Hepatocyte Growth Factor (HGF) necessary for the promotion of the liver phenotype.

Hydrogels with different volume ratios between the two polymers (GEL-ELR 100/0, 75/25, 50/50, 25/75, 0/100) were compared in terms of mechanical properties, Equilibrium Water Content (EWC), microstructure, heparin retention, and HGF retention.

The main hypothesis tested in this project was that the presence of ELR with heparin binding sites could increase the retention of HGF by the hydrogel.

The storage modulus at shear most similar to the native liver value reported in the literature was found to be 505 Pa for GEL-ELR 50/50.

The swelling ratio of the GEL-ELR 50/50 was calculated to be 5.1 ± 1.4, and microscopy images revealed that the mean pore area was 17 ± 4.64 μm^2.

The potential of the GEL-ELR to bind heparin and HGF was evaluated by analyzing the release profiles of these molecules over a 7-day period.

It was determined that the GEL-ELR 50/50 retained up to 95% of the loaded heparin and up to 77% of HGF.

These results represented a very promising outcome for future cellular studies with hepatocytes.

KEY WORDS hydrogel; gelatin; elastin; growth factor retention; hepatocyte

RESUMEN

Este proyecto tiene como objetivo demostrar el potencial del uso de un hidrogel innovador Gelatin-Elastin (GEL-ELR) como matriz para el cultivo de células hepáticas, con posibles aplicaciones para el estudio de la toxicidad de los fármacos.

El GEL, a través de sus dominios RGD, promueve la adhesión celular, mientras que el ELR aporta rigidez mecánica. Además, el ELR específico utilizado en este estudio contiene sitios de unión a heparina con afinidad a factores de crecimiento, para atraer el factor de crecimiento hepatocitario (HGF) necesario para la promoción del fenotipo hepático.

Se compararon hidrogeles con diferentes relaciones de volumen entre los dos polímeros (GEL-ELR 100/0, 75/25, 50/50, 25/75, 0/100) en términos de propiedades mecánicas, EWC, microestructura, retención de heparina y HGF.

La principal hipótesis probada en este proyecto fue que la presencia de ELR con sitios de unión a la heparina podría aumentar la retención de HGF por el hidrogel.

El módulo de almacenamiento a la cizalla más similar al valor del hígado nativo reportado en la literatura se encontró que era 505 Pa para GEL-ELR 50/50.

La relación de hinchamiento del GEL-ELR 50/50 se calculó en 5,1 $\pm$ 1,4, y las imágenes de microscopía revelaron que el área media de los poros era de 17 ± 4.64 μm^2.

Se evaluó el potencial del GEL-ELR para unir heparina y HGF analizando los perfiles de liberación de estas moléculas durante un periodo de 7 días.

Se determinó que el GEL-ELR 50/50 retenía hasta el 95% de la heparina cargada y hasta el 77% del HGF.

Estos resultados representan un resultado muy prometedor para futuros estudios celulares con hepatocitos.

PALABRAS CLAVE hidrogel; gelatina; elastina; retención de factor de crecimiento; hepatocito

RIASSUNTO

Questo lavoro mira ad caratterizzare l'impiego di un innovativo hydrogel Gelatin-Elastin (GEL-ELR) come matrice per la coltura di cellule epatiche, con potenziali applicazioni per i test di tossicità dei farmaci.

Sono stati confrontati hydrogel con differenti frazioni di volume tra due differenti polimeri (GEL-ELR 100/0, 75/25, 50/50, 25/75, 0/100) in termini di proprietà meccaniche, EWC, microstruttura, ritenzione di eparina e ritenzione di HGF.

L'ipotesi principale testata in questo progetto è che la presenza di ELR con siti di legame per l'eparina possa aumentare la ritenzione di HGF da parte dell'hydrogel.

Il modulo di accumulo al taglio più simile ai valori riportati in letteratura per il fegato nativo è risultato essere di 505 Pa per GEL-ELR 50/50.

Il rapporto di rigonfiamento del GEL-ELR 50/50 è stato calcolato pari a 5.1 ± 1.4 e le immagini al microscopio hanno rivelato che l'area media dei pori era di $17 \pm 4.64\ \mu m^2$.

Il potenziale del GEL-ELR di legare eparina e HGF è stato valutato analizzando i profili di rilascio di queste molecole per un periodo di 7 giorni.

È stato determinato che il GEL-ELR 50/50 ha trattenuto fino al 95% dell'eparina caricata e fino al 77% di HGF.

Questi risultati sono molto promettenti per futuri studi cellulari con gli epatociti.

PAROLE CHIAVE hidrogel; gelatina; elastina; fattori di accrescimento epatici; epatociti

ACKNOWLEDGMENTS

I would like to express my gratitude to everyone who helped me with suggestions, criticism and observations during this experience. I sincerely wish to thank Professor Gloria Gallego Ferrer, without whom my stay at *CBIT* would not have been possible, and Raquel for constantly supporting and teaching me during these months. In addition, I would also like to thank them for their valuable advice in the preparation of this work.

Moving on, I would like to thank all the *CBIT* staff for sharing their expertise with me and for their kindness. To all of you goes my sincerest gratitude.

Special thanks to my family, friends and colleagues at the university for their support over the years and for allowing me to reach this important milestone.

CONTENTS

LIST OF FIGURES

LIST OF TABLES

ACRONYMS

DILI Drug-induced Liver Injury

DMEM Dulbecco's Modified Eagle Medium

DMF Dimethylformamide

DSC Differential Scanning Calorimetry

ECM Extracellular matrix

EDC *N*-ethyl-*N'*-(3-dimethylaminopropyl)carbodiimide hydrochloride

ELR Elastin-Like Recombinamers

EWC Equilibrium Water Content

FESEM Field Emission Scanning Electron Microscope

GEL-ELR Gelatin-Elastin

GEL-TYR Gelatin-Tyramine

GEL Gelatin

GF Growth Factor

HGF Hepatocyte Growth Factor

HLA Human Leukocyte Antigen
HRP Horseradisch peroxidase
iPSCs Induced Pluripotent Stem Cells
MES 2-(*N*-morpholino) ethanesulfonic acid
MW Molar Weight
MWCO Molecular Weight Cut-off
NHS *N*-hydroxysuccinimide
NTP Notas Técnicas de Prevención
PBS Phosphate-Buffered Saline
RT Room Temperature
TYR Tyramine
VAT Value Added Tax

INTRODUCTION

0.1 BACKGROUNDS

GENEALOGY OF TISSUE ENGINEERING The idea of applying technical knowledge to heal the human body has accompanied man since ancient times. The use of materials to close wounds through suture has been known since the Neolithic period (10000 BC) and the materials ranged from synthetic (linen for the Egyptians), to natural (catgut by the Europeans) and biological (heads of large ants in the Indian subcontinent and South Africa) [1]. One of the first testimonies of the use of biomaterials as prosthesis comes from a mummified body discovered in Egypt (Figure 2), where the big toe of the right foot had been amputated and replaced with a wooden one [2].

Art history also takes a role in this context, the painting *A verger's dream: Saints Cosmas and Damian performing a miraculous cure by transplantation of a leg* (Figure 3) represents the first known leg transplant for the treatment of a cancer [4].

MODERN TISSUE ENGINEERING Moving on to modern times, in 1995 Langer et al. introduced the concept of *tissue engineering* as an interdisciplinary field that combines engineering and life sciences and *"may create opportunities to provide less costly therapies and therapies that can save and improve lives"* [5]. Since then, tissue engineering has made enormous progress: from the discovery of methods to generate Induced Pluripotent Stem Cells (iPSCs) [6], which awarded John Gurdon and Shinya Yamanaka the Nobel Prize in Medicine in 2012, to the development of new biomaterials and scaffolds capable of mimicking tissues and organs. A summary of tissue engineering progress in the past decade is shown on Figure 1.

DRUGS DEVELOPMENT Thanks to these innovations in health sciences, the possibility of curing diseases and improving patients' quality of life has improved exponentially. Since the late 1990s, spending on drugs has grown faster than spending on other major components of the healthcare system and enormous efforts have been invested in trying to develop new therapies and drugs [7]. The investment in research and development required to bring a new drug to market has been estimated at around USD 985 million [8] and, for some drugs, as high as USD 2.6 billion [7]. In addition, a growing ethical awareness of animal experimentation linked to increasing computational potential and technical knowledge are pushing research in this field towards a reduction of in vivo tests in favour of in vitro tests [9].

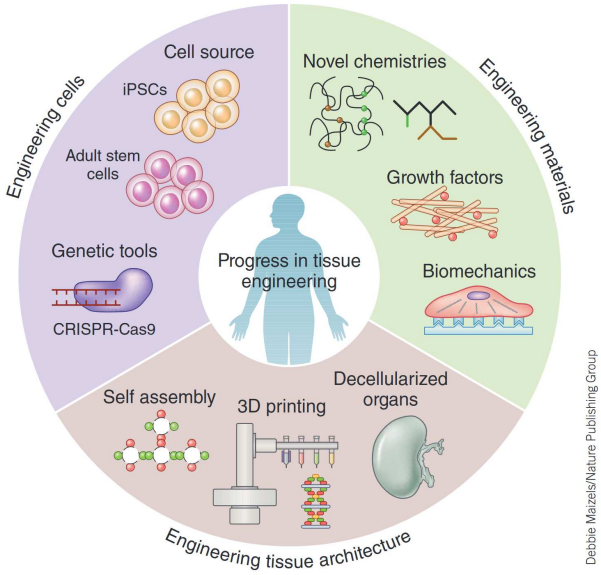

Figure 1: Summary of tissue engineering progress in the past decade. Adapted from [3]

Figure 2: Wooden prosthesis on an Egyptian mummy from 1550-700 BC.. Adapted from [2]

Figure 3: A verger's dream: Saints Cosmas and Damian performing a miraculous cure by transplantation of a leg. Oil painting attributed to the Master of Los Balbases, ca. 1495

0.2 MOTIVATIONS

This project, part of the final Master's project, was carried out at the Centre for Biomaterials and Tissue Engineering of the Polytechnic University of Valencia through the Erasmus+ project.

The reason for choosing the topic was a deep personal interest in the field of materials and their application in the area of tissue engineering. My personal vision of science is that it should have as its ultimate goal the improvement of human life and biomedical engineering best embodies this vision as it aims to improve health itself.

In this project, I had the opportunity to apply my theoretical knowledge in the field of polymers and gain practical knowledge of laboratory techniques that I had never experienced before.

In addition, I learnt and strengthened skills and knowledge such as:

- knowledge of tissue engineering, chemical synthesis and material properties;
- ability to work in a team, decision-making skills and knowledge of foreign languages;
- skills in scientific evaluation of results, graphic representation and public speaking

- bibliographic research and report writing skills

0.3 REGULATIONS

All experiments carried out in this project comply with current legislation in Spain.

The standards considered are mainly based on the classification and treatment of hazardous substances, labelling and waste management, as well as occupational safety and hygiene regulations.

In particular, some of the Spanish laws followed during the implementation of this project were:

- Real Decreto 374/2001. Protección de la salud y seguridad de los trabajadores contra los riesgos relacionados con los agentes químicos durante el trabajo
- Real Decreto 664/1997. Protección de los trabajadores contra los riegos relacionados con la exposición a agentes biológicos durante el trabajo
- Real Decreto 773/1997. Equipos de protección individual
- Real Decreto 952/1997. Normativa básica de residuos tóxicos y peligrosos
- Reglamento (UE) 2016/425. Equipos de protección individuals

Furthermore, although these are not mandatory standards, preventive technical standards should also be considered. Some of the *Notas Técnicas de Prevención (NTP)* followed during the project were:

- NTP 376. Exposición a agentes biológicos: seguridad y buenas prácticas de laboratorio
- NTP 432. Prevención del riesgo en el laboratorio-Organización y recomendaciones generales
- NTP 433. Prevención del riesgo en el laboratorio-Instalaciones, material de laboratorio y equipos
- NTP 663. Propiedades fisicoquímicas relevantes en la prevención del riesgo químico
- NTP 635. Clasificación, envasado y etiquetado de las sustancias peligrosas;

0.4 THESIS STRUCTURE

This work is conceptually divided into four parts: the first part has an introductory purpose and includes Chapter 1, where some notions

of liver tissue engineering are presented, and Chapter 2, which outlines the hypotheses and objectives of this project. The core part of the project covers the synthesis and characterization of gelatin-elastin hydrogels. Chapter 3 presents the materials and methods used, while Chapter 4 presents the results obtained and their comments. The third part of the project concerns a financial analysis: Chapter 5 details the cost of all reagents and methods used during the experiments performed. Finally, the last part provides the conclusions (Chapter 6) and possible next steps (Chapter 7).

Part I

INTRODUCTION

1 LIVER TISSUE ENGINEERING

Since this work regards the design and characterisation of hydrogels for liver cell culture, it is worthwhile to provide some basic anatomical background of the liver. In addition, the topic known as *Drug-induced Liver Injury (DILI)* is discussed. Moreover, this chapter presents an introduction to *in vitro model*, with a particular focus on *injectable hydrogels*. The last part is dedicated to the description of the two materials used during the project: Gelatin (GEL) and Elastin-Like Recombinamers (ELR).

1.1 LIVER

The liver represents the largest organ of the abdominal viscera and is located in the upper abdominal cavity, below the diaphragm, and above the stomach, right kidney, and intestines (Figure 4). It occupies most of the right hypochondrium and epigastrium and extends into the left hypochondrium to the left anterior axillary line [10]. Generally, the liver accounts for 2% of total body weight in adults, even if the size of it varies according to sex, being generally smaller in women [11] A representation of the anterior surface of the liver is given on Figure 5. The colour is reddish-brown, but may vary depending on the percentage of fat, assuming a more yellow tone [12].

1.1.1 *Structure*

Based on the external appearance, it is possible to identify four different areas in the liver, called *lobes*:

- right lobe: this is the largest lobe and extends over all the surface of the liver. It is divided from the left lobe by the falciform ligament anteriorly and superiorly and the ligamentum venosum and fissure for the ligamentum teres inferiorly [10];
- left lobe: this lobe has about half the volume of the right. It is thinner, and has a triangular shape;
- quadrate lobe: It is situated anterior to the porta hepatis and is bounded by the gallbladder fossa on the right, a short portion of the lower border anteriorly, the fissure for the ligamentum teres on the left, and the porta hepatis posteriorly [10];
- caudate lobe: this lobe lies posterior to the porta hepatis.

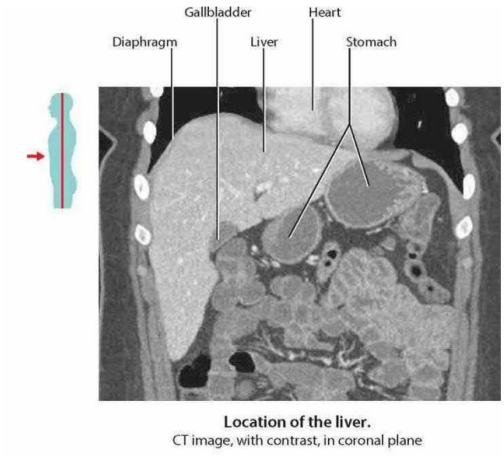

Figure 4: Location of liver. Adapted from [10]

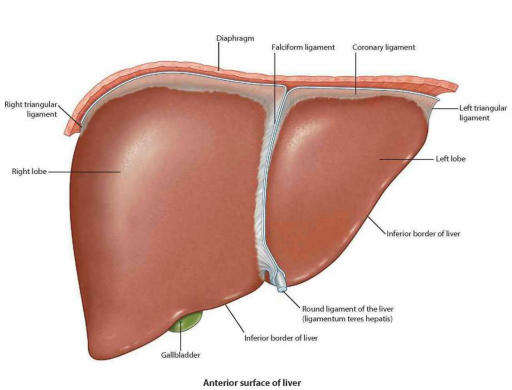

Figure 5: Anterior surface of liver. Adapted from [10]

The liver's surface is also divided into different fissures: three major fissures (main, left, and right portal fissures) and three minor fissures (umbilical, venous and fissure of Gans).

The liver is a very vascular organ and at rest condition receives up to 25% of total cardiac output [11]. These blood supplies are provided by two venous systems: the portal system and the hepatic system. The former transports venous blood from most of the gastrointestinal tract and its associated organs to the liver. The hepatic venous system, on the other hand, drains blood from the liver parenchyma into the inferior vena cava [10].

1.1.2 *Function*

The liver performs a wide range of metabolic activities required for homeostasis, nutrition, and immune defense [11]. It secretes a product called *bile* that helps carry waste products away from the liver. All blood coming out of the stomach and intestines passes through the liver to be filtered and then this organ processes this blood to obtain the nutrients needed by the body.

It also plays a key role in metabolising drugs into forms that are easier for the rest of the body to use or non-toxic [13].

Among the other functions, it is essential to regulate blood glucose and lipids, store specific vitamins, iron, and other micronutrients. Once the nutrients have been filtered out, its by-products are excreted in bile or blood. The by-products of bile enter the intestine and are expelled in the faeces, while the by-products of blood are first filtered by the kidneys and excreted through urine.

1.1.3 *Cells of the liver*

The liver cell population is vast and includes several cells. Among the principal cells, there are hepatocytes, hepatic stellate cells, sinusoidal endothelial cells, macrophages (Kupffer cells), the epithelial cells of the biliary tree (cholangiocytes), hepatic stem cells, natural killer lymphocytes (pit cells) [10].

HEPATOCYTES Hepatocytes are the primary liver cells, representing about 60% of the total cell population. These cells are characterised by a polyhedric shape with 5-12 sides and have a primary dimension of about 20-30 µm [10]. Their cytoplasm typically contains a considerable amount of rough and smooth endoplasmic reticulum, many mitochondria, lysosomes, and a well-developed Golgi apparatus, indicating high metabolic activity [10]. Hepatocytes are exposed to blood plasma, and the lateral plasma membranes of adjacent hepatocytes form microscopic channels: the bile canaliculi. Individual tight junction complexes are involved in signalling pathways in health

and disease [10]. It is also demonstrated that they play a fundamental roles in metabolism, detoxification, and protein synthesis. In fact, they are essential for innate immunity against bacterial infection by producing a wide variety of innate immunity proteins [14]

1.1.4 *Regeneration*

The liver is the only organ in the body capable of implementing regenerative mechanisms to ensure that the body's homeostasis is always at maximum efficiency [15]. It has been demonstrated that all hepatic cell types participate in cell proliferation during liver regeneration and this process is typically characterised by phenotypic fidelity, meaning that each cell is responsible for the regeneration of the same type of cells [15]. The mechanism of liver regeneration is still under investigation. A study on rats conducted by Michalopoulos and Bhushan [15] has shown that after a two-thirds partial hepatectomy, the portal vein undergoes a narrowing of its lumen by one-third of its original width. As a result, the pressure on the portal vein increases and this mechanism provides the initial signals for liver regeneration. Within 1 minute of partial hepatectomy in rats, there is an increase in the activity of urokinase-type plasminogen activator (uPA), which converts plasminogen to plasmin, in turn activating metalloproteinases and HGF. In less than an hour, this leads to a massive release of HGF, signalling molecules and other components of the hepatic Extracellular matrix (ECM) into the peripheral blood. Over the following few weeks, the new liver tissue becomes indistinguishable from the original tissue.

1.2 DILI

Drug-induced Liver Injury (DILI) is a term used to describe a liver injury suspected to be caused by chemical drugs. It represents the most common cause of acute liver failure in Europe and the USA: an estimated 139.0-240.0 per million of the world's population suffers from drug-induced hepatotoxicity each year [16].

DILI also accounts for the main reason for rejecting an investigational drug. This results in the failure of the clinical trials and, consequently, in a significant loss of investment, both in terms of money and time [16].

Generally, this pathology is referred to by differentiating two different cases:

- intrinsic DILI: refers to liver damage caused by drug overdose and occurs shortly after exposure. The primary example of intrinsic DILI is the assumption of acetaminophen, which is responsible for 50% of acute liver failure (ALF) cases in the US and some European countries [17].

- idiosyncratic DILI, refers to liver damage resulting from a drug used in the recommended daily doses. This reaction can be severe and, in some cases, also fatal [17].

While the former is relatively easy to predict, being caused by excessive drug intake, idiosyncratic-DILI is strongly linked to the genetic variable and is extremely difficult to predict [18].

The main explanation for the liver's susceptibility to adverse drug reactions is probably its central role in removing drugs from the circulation [17]. Drugs are uptake into hepatocytes either passively or trough transport proteins that are located in the basolateral plasma membrane. Then, drugs are metabolized by two enzymatic reactions: phase I and phase II. It is proved that a cause of DILI is the formation of reactive metabolites during phase I and II reactions [17]. Finally, drugs are expelled into bile for renal excretion. These reactive metabolites can bind covalently with cellular proteins, leading to the alteration of target protein function, or to the formation of immunogenic haptens, which can trigger an immune response.

However, the pathophysiological mechanisms of such reactions remaining poorly understood, and, consequently, there are currently no preclinical models to predict the toxicity of potential drug candidates [19]. Moreover, based on several genetic studies conducted, genetic factors seem to have a role in DILI. The main genetic factor that emerged as a significant risk factor is the association with specific Human Leukocyte Antigen (HLA) genotypes [20].

CURRENT MODELS The main difficulty in identifying drug toxicity is that there is no simple correlation between in vitro and in vivo drug activation [21]. Furthermore, human hepatotoxicity correlates poorly with regulatory toxicity tests on animals [22] and consequently these tests are not very predictive. Consequently, also considering the genetic component of this disease, a new approach based on personalised medicine integrating bio-informatics and tissue engineering is needed. In this context, the development of a scaffold that closely mimics liver conditions and can envelop patient-specific cells could represent an optimal in vitro test for patient-specific drug toxicity. Among scaffolds, hydrogels are prominent candidates.

1.2.1 *Hydrogels*

Hydrogels are materials that present an excellent biodegradability and biocompatibility and are gaining a major role in tissue engineering [23]. They are 3D solid structures formed by the cross-linking of hydrophilic polymeric chain network. Their main characteristic is the capability of retaining a significant amount of water remaining insoluble in water, given by the incorporation of hydrophilic functional groups as –NH2, –CONH, –COOH [24]. Hence, a cross-linked poly-

mer hydrogel swells but does not dissolve when water or a solvent enters it.

Hydrogels can be classified into two wide groups according to the types of polymers they are composed of:

- natural polymers: this group refers to all the polymers that can be found in nature;
- synthetic polymers: this group refers to polymers that are artificial synthesised.

Generally speaking, natural polymers present better biocompatibility, while synthetic ones are more tunable as they can modified ad hoc to obtain the desired properties [25].

Another differentiation between hydrogels can be done basing on the cross-linking methods, that can mainly be physical or chemical:

- physical crosslinking: is usually based on intramolecular reversible interactions and can involve several mechanisms like heating or cooling the polymer solution, ionic interaction, H-bonding;
- chemical crosslinking is based on embedding of monomers on the chains of the polymers or the use of cross-linking agents to create a linkage between polymers.

The main difference is that physical mechanisms do not require a chemical reaction, thus avoiding possible toxic interactions with cells. However, if it is a thermal process, cross-linking must be carried out at a temperature of 37 °C for cells not to be damaged. Furthermore, physical cross-linking is less stable than chemical cross-linking, and while the former is reversible, the latter relies on the creation of irreversible covalent bonds. On the other hand, chemical reagents may be toxic for an application in cell culture. Therefore, none is better than the other, and the selection depends on the objective to be achieved.

For what regards tissue engineering applications, these materials are perfect candidates for drug delivery as present a highly porous structure where drugs can be incorporated [23].

However, the application of pre-formed hydrogels in the body demands an invasive surgical procedure and does not allow the perfect adhesion to the specific sites [26]. For this reason, the used of preformed hydrogels during clinical trials is reduced and they are replaced by *injectable hydrogel* [25].

The term *injectable hydrogel* refers to a hydrogel that can be injected with minimal invasiveness into target sites and used for irregularly shaped sites.

The first tissue engineering application of injectable hydrogels was presented in 1990 by Elisseeff et al. with a study on the transdermal

polymerizationon of polyethylene oxide (PEO) [27] [25] and, so on, these polymers have been applied to many different fields.

The high tunability of these polymers allows for strict control of the rate of degradation and, since they can be formed directly in situ after injection into the body, they have also begun to take on a predominant role as delivery systems for therapeutic agents [25].

For what regards in vitro hydrogel for liver studies, the main materials that have been used are hyaluronic acid, chitosan, alginate, gelatin [28]. Just as an example, Xu et al. studied injectable hyaluronic acid-tyramine hydrogels for liver cancer therapy [29], while Zhou et al. worked with injectable chitosan-based hydrogels for drug delivery [14]. Sanmartín-Masiá, Poveda-Reyes, and Ferrer synthesised and characterised an injectable gelatin-hyaluronic acid hydrogel [30], while Rajalekshmi et al. studied fibrin (FIB) incorporated injectable alginate dialdehyde (ADA) - gelatin (G) hydrogels [31]

1.3 GELATIN

One of the most common materials employed for hydrogels is gelatin, a protein produced by the partial denaturation or hydrolytic degradation of collagen [32].

There are many resources from which it is obtained, such as animal skin, bone or connective tissue [24]. Since it does not exist in nature, gelatin is classified as a derived protein and is usually divided into two groups [24]):

- type A gelatin: is produced from collagen using acidic chemical agents such as hydrochloric acid or sulphuric acid;
- Type B gelatin is obtained from collagen through alkaline or lime-based processing.

The most advantageous properties of gelatin are related to the excellent biocompatibility, and non-cytotoxicty [33]. In fact, it is derived from collagen, which is one of the fundamental proteins that make up ECM.

With regard to mechanical properties, gelatin scaffolds exhibit weak stress resistance. However, it is possible to increase these by crosslinking mechanisms, by synthesising hydrogels with a higher polymer content or by combining it with other polymers, such as hyaluronic acid as shown in [30].

Another relevant property is the porous structure of the gelatin hydrogels, which provides the necessary space for cell adhesion, thus making cell-material interactions possible.

Referring to thermal behaviour, the upper critical temperature of the solution is around 30 °C. Below this temperature, inter-molecular hydrogen bonds form in a reversible process that induces gelation [32].

Regarding hydrogels for liver tissue engineering, gelatin has been used mainly in combination with other polymers to achieve optimal properties. Because these combinations of materials open the door to enormous possibilities, a vast amount of different gelatin-based hydrogels can be found in the literature.

As an example, Luetchford, Chaudhuri, and De Bank decided to combine gelatin with silk fibroin, achieving higher mechanical and cytocompatibility properties [34]. The authors also showed that the degradation rate was controllable through the ratio of gelatin.

Sanmartín-Masiá, Poveda-Reyes, and Ferrer worked with hydrogels of hyaluronic acid and gelatin at different volume ratios and demonstrated that an increase in the fraction of hyaluronic acid increased mechanical properties [30]. Yang et al. studied the influence of different crosslinking mechanism to gelatin sponge scaffolds, obtaining highly biocompatible hydrogels [33].

CELLS-MATERIAL INTERACTION The interaction between material and cells is crucial for regulating cell adhesion, migration, growth and differentiation.

Integrins are a class of trans-membrane cell receptors, composed of an α sub-unit and a β sub-unit, that mediate cell-cell and cell-ECM interactions. Therefore, the interaction between integrins on cells and particular sequences on the surface of materials is a crucial factor in regulating cell biology.

Gelatin (GEL), as well as collagen from which is derived, contains in its sequence the linear RGD (Arg-Gly-Asp) cell adhesive motif, that represent a major recognition system for cell adhesion [35]. This motif was found in fibronectin in 1984 for the first time and the authors concluded that it *"may constitute a cellular recognition determinant common to several proteins"* [36]. Since then, numerous studies have been conducted that have demonstrated the enormous potential of RGD domains in binding various integrins and, in particular, $\alpha_5\beta_1$ and $\alpha_v\beta_3$ integrins [37]

Therefore, the use of gelatin ensures the adhesion of cells to the hydrogel, which is the first step towards the ultimate goal of mimicking the natural liver environment.

In addition, Ozeki and Tabata showed that Gelatin type A has an affinity for HGF related to hydrophobic and hydrogen bonding interactions [38].

1.3.1 *Gelatin-Tyramine modification*

Gelatin can be modified with tyramine hydrochloride to introduce phenolic groups into the chains and allow subsequent hydrogel formation by enzymatic reaction with Horseradisch peroxidase (HRP) and H_2O_2.

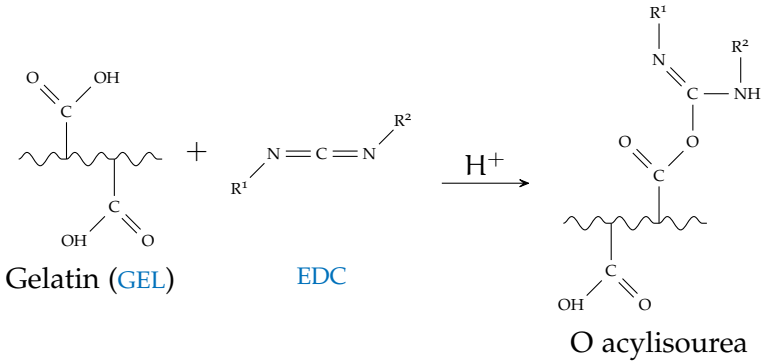

Figure 6: Reaction of the carboxylic acid of gelatin with a water-soluble carbodiimide with the formation of an O acylisourea. Adapted from [39]

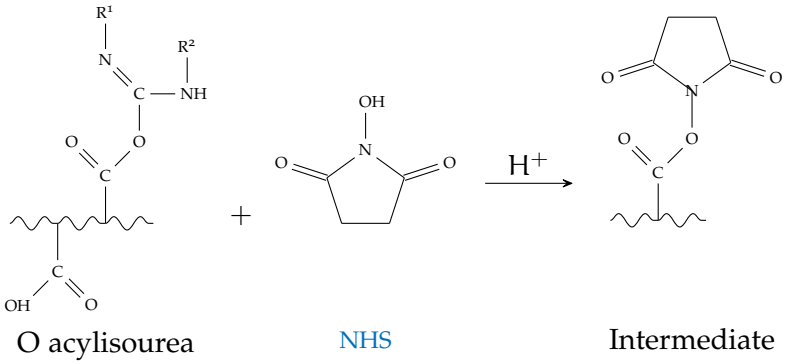

(a) Reaction of O-acylisourea with NHS with the formation of an intermediate. Notice that additional products have not been represented in this scheme

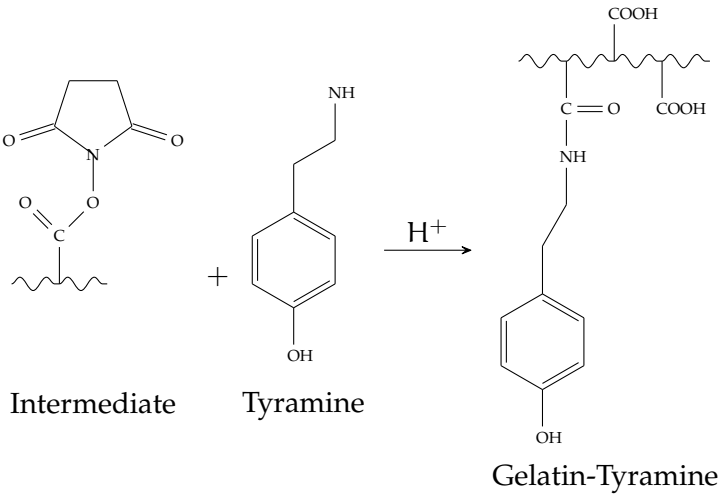

(b) Reaction of the intermediate with the phenol groups of the tyramine, obtaining modified gelatin

Figure 7: Scheme of the reaction of O-acylisourea with NHS and tyramine giving rise to the tyramine graft in the chains of gelatin. Adapted from [39]

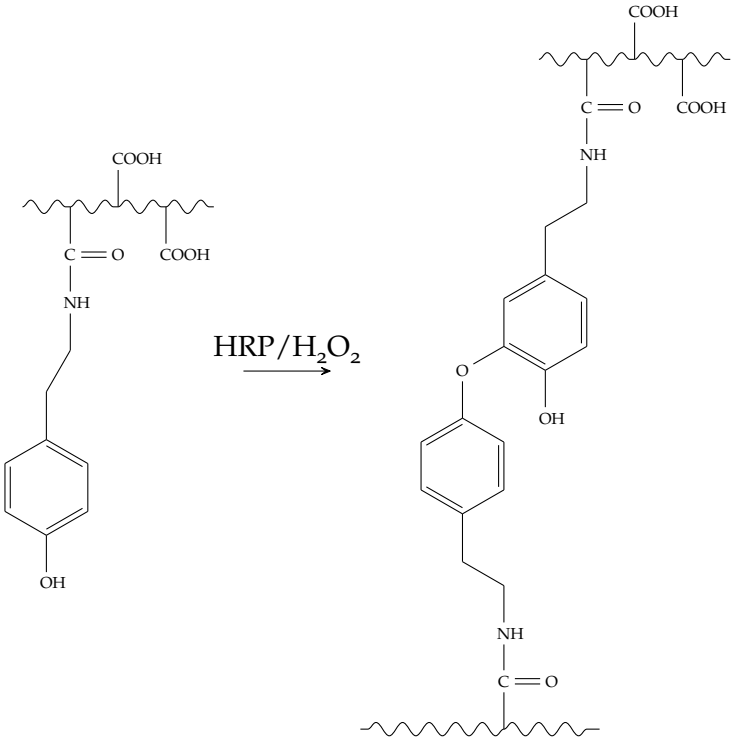

Figure 8: Scheme of the enzymatic crosslinking reaction of Gelatin in presence of HRP and H_2O_2. Adapted from [40]

In this project, tyramine grafting was obtained by combining gelatin from porcine skin type A and tyramine hydrochloride via the carbodiimide-mediated condensation of the carboxyl groups of gelatin and the amino groups of tyramine Figure 1.3.1 [40]. *N*-hydroxysuccinimide (NHS) and *N*-ethyl-*N*'-(3-dimethylaminopropyl)carbodiimide hydrochloride (EDC) were used as stabilizer and catalyst of the reaction respectively. The initial phase is the reaction of the carboxylic acid of gelatin with a water-soluble carbodiimide, that involves the formation of an O-acylisourea as reported in Figure 7 [39]. Then, O-acylisourea reacts with tyramine and NHS to form an amide bond giving rise to the modification of gelatin chains with the introduction of the phenol groups.

1.3.2 *Gelatin hydrogel formation*

The chemical cross-linking of GEL hydrogels was achieved by means of an oxidative coupling reaction by the enzyme HRP and hydrogen peroxide (H_2O_2) [40]. The reaction takes place in two stages. First, HRP is oxidised in the presence of H_2O_2 to form an intermediate that thereafter oxidises the phenolic groups of the tyramine grafted into gelatin resulting in cross-linking of the hydrogel. A schematic of the chemical structure of the hydrogel obtained after the enzymatic with HRP and H_2O_2 is shown in Figure 8

1.4 ELASTIN

Elastin is a protein that represents one of the most important components of vertebrate ECM. It is a highly insoluble polymer composed of covalently cross-linked molecules of its precursor tropoelastin, a soluble, non-glycosylated and highly hydrophobic protein [41]. The primary elastin sequence presents regions governed by repeated amino acid patterns, such as VPGG, VPGVG, APGVG and VGVAPG. [42]. Their structure allows elastin molecules to undergo significant deformation without breaking and to return to their original conformation once the stress disappears, giving the elastic properties that characterise elastin [42]. In addition to providing elasticity to tissues, it plays a role in promoting tissue repair and regulating cell behaviour inducing specifics responses [41]. A particular property of elastin is *coacervation*, a self-aggregation process in which the protein comes out of solution as a second phase on a rise in the temperature of the solution [43]. This property characterises also Elastin derived polymers, such as ELR that will be discussed in following section.

1.4.1 *Elastin like recombinamers*

In recent years, the application of powerful molecular biological methods has enabled the design and synthesis of new advanced materials based on the combination of 20 naturally occurring amino acids. These materials exhibit some properties present in natural proteins, but allow the advantage of a full degree of control provided by genetic engineering.

In the literature, there are many terms used to refer to such materials; however, according to Rodríguez-Cabello et al. [42], the best term is *Recombinamer*. This term, in fact suggests a molecule whose composition is strictly defined by engineering design.

Among these materials there are Elastin-Like Recombinamers (ELR): biocompatible protein-based polymers which are based on a repeat sequence found in elastin. The primary sequence of ELR is typically governed by n repeats of the amino acidic sequence (VPGXG), where X is any amino acid except L-proline [44].

Thanks to the advanced genetic engineering techniques now possible, these materials can be synthesised with tight control over several important parameters, such as chain length, stechiometry or chain substitution.

They also benefits from the properties proper of elastin, since the host organism's immune system is unable to distinguish between endogenous elastin and an ELR [44]. Thus, ELR are characterised by extraordinary compatibility, high cells interaction and tissue mimetic mechanical properties.

Two different ELR were used in the project: VKV-24 and HBD6.

Figure 9: Amino acid structure of HBD6.

1.4.1.1 *VKV-24*

VKV-24 is a structural ELR that does not have any bioactive sequence and present the amino acid sequence: MESLLP VG VPGVG [VPGKG(VPGVG)5]23 VPGKG VPGVG VPGVG VPGVG [45]. Particularly relevant is the presence of the amino group ϵ in the lysine side chain (amino acid K), which is needed to bear functional groups such as cyclooctine and azide groups allowing crosslinking.

1.4.1.2 *HBD6*

The amino acid sequence of the HBD6 ELR, also defined as heparin-binding ELR, is given by the structure represented in Figure 9. The basic structure can be distinguished into seven blocks and is repeated six times in the final ELR composition.

ELASTIN-LIKE BLOCK: The block VPGIG is repeated four times and has the main function of giving the polymer the properties of elastin;

CROSS-LINKING BLOCKS: The block VPGKG is repeated two times and has the main function of conferring mechanical stability to the structure and allowing the crosslinking between chains. In particular, the presence of the lysine residue in the fourth position allows to modify the amine group of the side chain of the amino acid for crosslinking purposes;

BIO-ACTIVE REGION: The block PRRARV gives heparin-binding activity to the polymer

1.4.1.3 *Chemistry crosslinking*

The expression *click chemistry* was first introduced by Sharpless and Kolb to denote modular reactions, which give very high yields, generate only inexpensive products and are more stereo-specific [47], [46]. The 1,3-dipolar cycloaddition of organicazides and alkynes was first described by Huisgen in 1960 [48], while in 1961 Wittig reported that cyclooctene and phenylazide react extremely rapidly at Room Temperature (RT) to form a single product [49].

Based on these findings, Agard, Prescher, and Bertozzi developed a catalist free reaction that involved a cyclooctynes and an azide group,

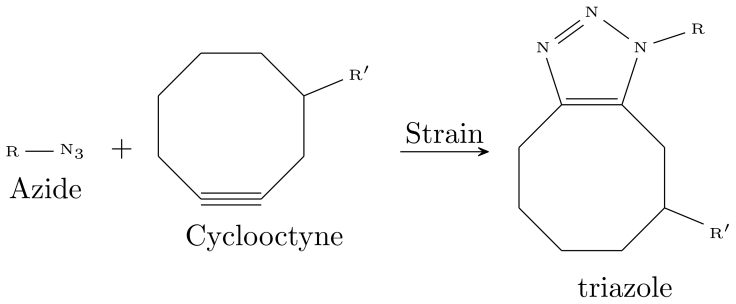

Figure 10: Strain-promoted cycloaddition of azides and cyclooctynes to form triazole products. Adapted from [46].

called Strain-promoted alkene-azide cycloaddition (SPAAC) [50] (Figure 10).

Due to the tension of the triple bond, the cyclooctyne have a distorted geometry that significantly lowers the activation energy and can react with the phenyl azide giving a single product named *triazole*. [46]. No negative effects on cell viability were observed during this reaction [50], making it a perfect candidate for biological applications.

In our project, the ELR were modified by introducing the two different functional groups required for the SPAAC reaction. An activated alkene was introduced in half of the molecules, while an azide group was introduced in the remainder.

1.5 CELLS-MATERIAL INTERACTION

One of the greatest challenges in tissue engineering is the adaptation of biomaterials to mimic the targeted phenotype. The key to achieving the desired properties is the control of the cellular environment, with the possibility of influencing cell differentiation and activity.

Cell-material interaction is a crucial aspect of material biocompatibility and is critical to properly mimic the specific phenotype. When a material is brought into contact with a fluid that contains soluble proteins, such as cell culture media, the proteins are rapidly adsorbed onto the surface of the material. On the other hand, when cells are in contact with the material, the larger size affects their mobility and, as a result, they do not interact with the molecular structure of the surface of the material itself, but rather with the molecular structure of the adsorbed protein layer [51]. The interaction between cells and material is based on the binding between membrane receptors and specific bio-active characteristics presented on the adsorbed proteins.

It is known that cells influence their environment (ECM) and vice versa by communicating through cell surface receptors. A key role

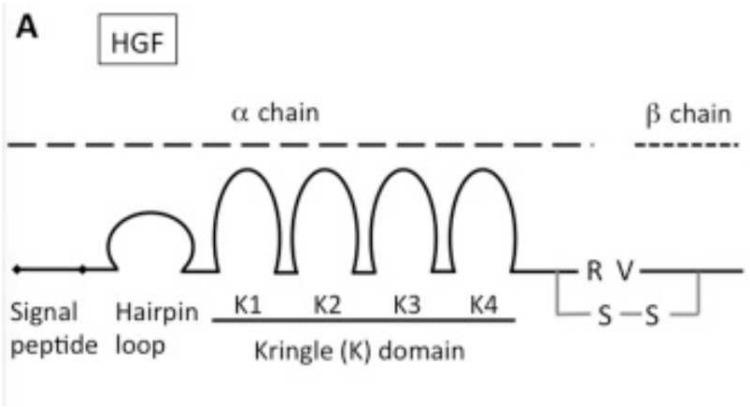

Figure 11: HGF structure. Adapted from [55]

in this interaction is played by integrins, which are trans-membrane receptors that connect the cytoskeleton with the extracellular environment [52]. The integrins are formed by two sub-units, called α and β, and bind specific ligand peptides in the ECM. One of the well-known interactions is that between the integrin $\alpha_v\beta_3$ and the RGD sequence. After this binding, the integrins form a group called focal adhesion, characterised by the presence of many structural and signalling molecules that bind the ECM to the cytoskeleton. Through this complex structure, cells are able to communicate with the environment and physical signals, such as stiffness, are converted into signalling cascades.

1.5.1 *Growth factors*

Growth Factor (GF) are soluble-secreted signalling polypeptides that facilitate localized and spatially regulated signaling instructing specific cellular responses [52]. These molecules have a strong and broad influence on cells, promoting their stimulation, proliferation, migration and differentiation [53]. In particular, GF plays a crucial role in cell-material interaction, regulating the signaling cascade and promoting the development of the desired phenotype.

Thus, when integrins and growth factor receptors are activated synergistically an enhanced effect of the growth factors is observed and very low dose of GF are required to stimulate the correct phenotype [52].

There is a wide variety of GF, with a wide diversity of biological results; among the most popular in tissue regeneration are: Ang (Angiopoietin), BMP (Bonemorphogenetic protein), EGF (Epidermal growth factor), FGF (Fibroblast Growth Factor), HGF (Hepatocyte Growth Factor) [54].

HGF HGF constitutes the most potent mitogen for mature hepatocytes in primary culture [55]. This protein is secreted by mesenchy-

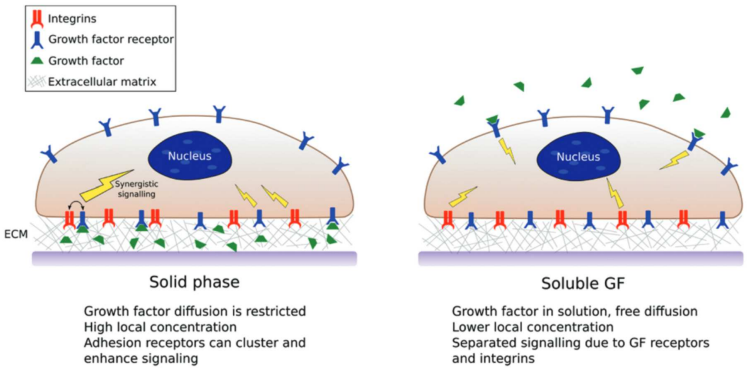

Figure 12: Main differences between soluble vs. solid-phase presentation of GFs. Adapted from [52]

mal cells and has many epithelial-derived functions in angiogenesis, tumorogenesis and tissue regeneration [56]. The coding gene is located on the seventh chromosome (7q21) at position 8169,905 - 81777150, and consists of 18 exons [57]. The exons encode the α chain, which consists of four kringle structures (triple disulphide loop structures), a small β chain and an intermediate region [56]. A representation of the molecular structure of HGF is shown in Figure 11. The α sub unit has a molecular weight of 69000 Da, while the β subunit of 34000 Da, for a total molecular mass of 82000 Da [55].

The receptor for HGF has been identified as a *c-met* protooncogene (MET), which upon binding to HGF is activated inducing various biological responses, including proliferation, cell survival, morphogenesis and angiogenesis. [56].

GF PRESENTATION There are two main mechanisms of GF presentation: soluble GF and solid-phase GF. Figure 12 schematize the main differences between the two methods.

The first method is based on the addition of GF directly into the culture medium or by release from a carrier, but this method does not replicate the in vivo condition, where GF are bound to the ECM [52].

Therefore, a more effective method is the solid-phase presentation of GF, as it better replicates the natural condition and gives enhanced biological function with lower doses used [52].

This method is based on the immobilisation of GF on the surface of the biomaterial and an effective strategy to achieve this binding is the use of heparin-binding domains.

Indeed, GF can be immobilised on the ECM due to their affinity for specifically introduced heparin-binding domain [53].

Therefore, introducing heparin into the material is an efficient mechanism to enhance the affinity with GF.

2 HYPOTHESIS AND OBJECTIVES

2.1 HYPOTHESIS

The aim of this work is to demonstrate the potential of using a novel Gelatin-Elastin (GEL-ELR) based hydrogel as a matrix for the culture of liver cells, with future applications as drug toxicity testing platform.

The hydrogel developed is an injectable in situ gelling hydrogel that employs non-toxic reactions to encapsulate Hepatocyte Growth Factor (HGF).

The composition of the hydrogel combines Gelatin (GEL), a protein derived from collagen and naturally present in the Extracellular matrix (ECM), and Elastin-Like Recombinamers (ELR), polymers engineered from elastin and widely adaptable.

The choice of combining these materials is based on the consideration that GEL, through its RGD domains, promotes cell attachment, whereas ELR provides mechanical stiffness. Furthermore, the chosen ELR has affinity to heparin and can attract the HGF to promote the liver phenotype.

It is necessary to study the mechanical properties at different concentrations and verify whether these are in line with the properties of the liver under natural conditions.

In addition, the ability of hydrogels to attract HGF is desired to present the Growth Factor (GF) from the solid phase and at low dose. Since the literature shows that heparin acts as an affinity site for HGF, high heparin retention is expected to be linked to high HGF attraction. For this purpose, two different ELR were used, named VKV-N_3 and HBD6-N_3. Both mimic the structure of natural elastin, but the latter has heparin-binding sites in its chains. Consequently, higher heparin retention is expected in hydrogels synthesised with HBD6-N_3 than in those with VKV-N_3 (used as negative control). Analogously, the highest HGF attraction is expected in hydrogels synthesised with HBD6-N_3.

2.2 OBJECTIVES

The main objective of the project is to obtain a scaffold that mimics the natural conditions of the liver, demonstrating the potential of using a novel gelatin-elastin-based hydrogel as a culture system for hepatic cells.

The hydrogels will be synthesised with different percentages of the two components, i.e. 100/0, 75/25, 50/50, 25/75, 0/100. In this way, it will be possible to determine which percentage has the mechanical properties closest to the native liver tissue.

The Equilibrium Water Content (EWC) of the hydrogel will be determined to characterize it.

Furthermore, the ability of hydrogels to attract Hepatocyte Growth Factor (HGF) will be determined.

Since the literature shows that heparin acts as an affinity site for HGF, high heparin retention is expected to be related to high HGF attraction. Therefore, the cumulative retained value of heparin will initially be determined by means of fluorescence techniques. Once any retention of heparin is established, HGF will be introduced into the hydrogel in order to quantify affinity.

Part II

SYNTHESIS AND CHARACTERISATION OF GELATIN-ELASTIN HYDROGELS

3 MATERIALS AND TECHNIQUES

This section provides a list of the reagents and instruments used during the synthesis and characterisation of hydrogels. In addition, the protocols applied during the various stages of the project are presented.

3.1 GELATIN-TYRAMINE SYNTHESIS

Gelatin was modified with tyramine inserts to introduce phenol groups: when tyramine is bound to gelatin chains, phenol groups are introduced into the chains and react with Horseradisch peroxidase (HRP) and hydrogen peroxide (H_2O_2) to form an hydrogel. The protocol used for the synthesis of Gelatin-Tyramine (GEL-TYR) was defined by [58] and was performed several times to obtain the polymer needed for different experiments.

3.1.1 *Materials*

The following materials and reagents from Sigma-Aldrich (Germany) were used for the synthesis of GEL-TYR:

- gelatin from porcine skin (type A, strength 300);
- NHS ($\geqslant$ 98%);
- tyramine hydrochloride ($\geqslant$ 98%);
- 2-(*N*-morpholino) ethanesulfonic acid (MES) ($\geqslant$ 99%),;
- EDC from Iris Biotech GmbH (Germany);
- dialysis membrane 12400 Molecular Weight Cut-off (MWCO);
- milliQ water

3.1.2 *Protocol*

The protocol followed for the synthesis of GEL-TYR polymer was proposed by [58]. The logical steps and calculations performed in order to determine the reagent quantities are presented in Appendix A. Since this protocol covers several work days, for the sake of readability, the steps are reported divided by workdays.

Day 1

First, 400 mg of gelatin and 195.24 mg of MES were added to 20 mL of milliQ water and dissolved for 30 min at 60 °C under stirring. Next, 111.13 mg of tyramine hydrochloride were added and allowed to dissolve for 20 minutes at Room Temperature (RT) under stirring. Then, the pH of the solution was adjusted with 0.1 M NaOH to 6. Next, 7.36 mg NHS was added to the solution and allowed to dissolve for 30 minutes at RT under stirring. Finally, 122.68 mg EDC were added to the solution and stirred for 24 h at 37 °C.

Day 2-Day 3

Next, the solution was dialysed against 2.5 L of deionised water for 48 h using a 12400 MWCO dialysis membrane. The water was changed three times per day, approximately with an interval of 4 hour.

Day 4

The solution was then poured into plastic containers, keeping in mind that the height of the solution in the plastic container should not exceed 1 cm. The solution was frozen at -80 °C for 24 h.

Day 5-6-7-8

The solution was freeze-drying at -80 °C in LyoQuest-85 from Telstar (Japan) for four days. The lyophilised GEL-TYR was finally stored in sealed jars with silica, ready to be used for the synthesis of hydrogels.

3.2 ELASTIN LIKE RECOMBINANTS SYNTHESIS

3.2.1 *Materials*

Regarding ELR, there was no need for synthesis as they were already produced by the *Bioforge Research Group* at the *University of Valladolid* (Spain).

As discussed in Section 3.2, two different polymers were needed to obtain the hydrogel: cycloctine-modified elastin (VKV-CC) and azide-modified elastin. For the latter, two different compounds were used, named VKV-N_3 and HBD6-N_3.

3.2.2 *Protocols*

As the synthesis of the polymers was performed by the *Bioforge Research Group*, it will not be discussed in detail in this work. More information about the process can be found at [45].

3.3 HYDROGELS SYNTHESIS

3.3.1 *Materials*

The reagents used for the synthesis of pure GEL-TYR and ELR-based hydrogels and different blends include:

- GEL-TYR, produced as described in Section 3.1.2
- ELR, which were a gift from the University of Valladolid as described in Section 3.3.2.2 ;
- Dulbecco's Modified Eagle Medium (DMEM), low in glucose, with sodium pyruvate, without glutamine or phenol red, from Thermo Fisher Scientific (USA);
- HRP (type VI) from Sigma-Aldrich (Germany);
- hydrogen peroxide (H_2O_2), 30% w/w solution in H_2O from Sigma-Aldrich (Germany).

3.3.2 *Protocols*

All the hydrogels synthesised and utilised through this project, were prepared with a concentration of 8% w/v (80 mg/mL)).

3.3.2.1 *GEL-TYR pure hydrogels*

GEL-TYR was synthesized as described in Section 3.1.2 and stored at RT in a jar sealed with silica. Then, it was dissolved in DMEM for 1 h at 37 °C. The amount of added DMEM was set to obtain an 8% w/v solution. Meanwhile, fresh solutions of HRP 12.5 U/ml and H_2O_2 (20 mM) were prepared in DMEM. HRP and H_2O_2 were stored in a refrigerator at 4 °C. After complete dissolution of GEL-TYR, the hydrogels were formed by first mixing 80% v/v of GEL-TYR solution and 10% v/v of HRP solution working at RT. Then, the solution was thoroughly but rapidly stirred doing up and down being careful not to create air bubbles. Finally, it was transferred to a mold and then the 10% v/v H_2O_2 solution was added dropwise.

The exact volumes of the reagents are listed on Appendix C.

3.3.2.2 *ELR pure hydrogels*

As discussed in Section 3.2, ELR were provided lyophilised by the *Bioforge Research Group* at the *University of Valladolid (Spain)*. First, HBD6-N3 and VKV-CC were dissolved in DMEM overnight at 4 °C. The amount of added DMEM was set to obtain an 8% w/v solution. It was crucial to work at a low temperature because above the transition temperature a conformational reorganisation would occur at

Figure 13: Mini fridge used for the synthesis of hydrogels at 4 °C

the molecular level, creating a solid phase [45]. The following day, the hydrogels were formed by mixing 50% v/v HBD6-N_3 or VKV-N_3 and 50% v/v VKV-CC solutions keeping working for the reason mentioned above at 4 °C in a fridge specifically modified (Figure 13). The solution was stirred thoroughly but rapidly, being careful not to create air bubbles. Finally, the mixed solution was transferred to the mold. The gelation time was approximately 10 minutes.

The exact volumes of the reagents are listed on Appendix C.

3.3.2.3 *GEL-TYR - ELR based hydrogel*

GEL-ELR 8% w/v hydrogels represented the most challenging task to synthesise as Gelatin (GEL) gels at temperatures below 20 °C, while Elastin-Like Recombinamers (ELR) at temperatures above 10 °C. Consequently, several protocols had to be tested to find the best one.

Firstly, HBD6-N_3, VKV-N_3 and VKV–CC were dissolved in DMEM overnight at 4 °C. The amount of added DMEM was set to obtain an 8% w/v solution. The next day, gelatin synthesised as described in Section 3.3.2.1 was dissolved in DMEM for 1 h at 37 °C to create an 8% w/v solution. Meanwhile, fresh solutions of HRP (12.5 U/ mL^{-1}) and H_2O_2 (20 mM) in DMEM were prepared analogously to synthesise pure GEL-TYR hydrogel. In order to prevent the ELR from gelling, the hydrogel synthesis took place at 4 °C operating in the specially modified refrigerator shown in Figure 13. All reagents and necessary instrumentation (molder, tubes, micropipette tips) were stored at 4 °C from the previous night. An exception was the gelatin, which was kept at RT.

To form the hydrogels, the following sequence was followed:

1. put 25% v/v VKV-N_3 solution (or HBD6-N_3 solution) into an Eppendorf tube;
2. add 5% v/v HRP solution;
3. add 25% v/v VKV-CC solution, mixing carefully but fasting in order to avoid gelification;
4. transfer the solution into the moulder;
5. add 40% v/v gelatin solution;
6. add 5% v/v H_2O_2.

The exact volumes of the reagents are listed on Appendix C.

NOTE For ease of reading, the term GEL hydrogels will be used instead of GEL-TYR hydrogels on the following pages. In each application, however, the gelatin used was modified with tyramine.

3.4 SWELLING BEHAVIOUR TEST

The determination of the Equilibrium Water Content (EWC) is essential for characterising a hydrogel as it is a parameter closely linked to many other properties. Generally, a higher water retention is more advantageous for medical applications as it indicates higher permeability and biocompatibility of hydrogels [59]. On the other hand, mechanical properties decrease with high water absorption, so a good compromise has to be found. A good solution is to copolymerize a hydrophilic monomer (which promotes swelling) with a less hydrophilic monomer. In this way, a hydrogel with good water absorption and better mechanical properties can be obtained [59].

3.4.1 *Materials*

- Hep2G medium of culture

3.4.2 *Methods*

The different types and volumes of reagents used for the hydrogel synthesis are shown in Appendix C. Once made, they hydrogels were weighed to obtain the *fresh weight* (m_0). They were subsequently immersed in Hep2G medium for 24 h at 37 °C. Later, they were weighed a second time to obtain their *wet mass* (m_w). Then, the hydrogels were frozen using liquid nitrogen, lyophilised overnight and weighed again to obtain their *dry mass* (m_d).

The swelling behaviour of the hydrogels was characterised by calculating the swelling ratio, defined in Equation 1.

$$EWC = \frac{m_w - m_d}{m_d} \tag{1}$$

3.5 FIELD EMISSION SCANNING ELECTRON MICROSCOPY

3.5.1 *Materials*

- Hep2G medium
- liquid nitrogen
- sharp blade
- adhesive carbon black
- platinum coating

3.5.2 *Methods*

The morphology of the hydrogels was characterised via Field Emission Scanning Electron Microscope (FESEM) (GeminiSEM 500, ZEISS, Germany) with an operating voltage of 1.5 kV. This instrument allows obtaining a detailed image of the sample surface by scanning with a highly focused beam of high- and low-energy electrons [60].

The hydrogels were prepared two days in advance and soaked for 24 h in Hep2G medium at 37 °C. They were then frozen with liquid nitrogen and lyophilised at -80 °C overnight. Hence, the lyophilised hydrogels were cut with a sharp blade to obtain their cross-sections. The samples were then mounted on adhesive carbon black and coated with platinum.

3.6 RHEOLOGICAL MEASUREMENTS

Rheometry is a technique for measuring the shear deformation of a viscoelastic material when a certain shear stress is applied.

In a viscoelastic material, unlike an elastic material, the properties are a function of strain frequency, and one of the most common methods to characterise the viscoelastic properties of soft tissue is the *frequency sweep test* [61].

In this experiment, the top plate of the rheometer oscillates at varying frequencies (ω) with an amplitude of γ_A with the aim of introducing a sinusoidal shear stress, γ^*

$$\gamma^* = \gamma_A e^{i\omega t} = \gamma_A \sin \omega t \tag{2}$$

Throughout the oscillation, the reaction torque is measured and the complex shear stress τ^* is calculated:

$$\tau^* = \tau_A e^{i\omega t+\delta} = \tau_A \sin \omega t + \delta \tag{3}$$

Where τ_A is the amplitude of the shear stress and δ is the phase angle. Finally, the complex modulus G^*, the storage modulus $G^{'}$ and loss modulus $G^{''}$ are calculated:

$$G^* = \frac{\tau^*}{\gamma^*} \tag{4}$$

$$G^* = G^{'} + iG^{''} \tag{5}$$

3.6.1 *Materials*

- Discovery HR-2 Hybrid rheometer from TA Instruments (USA)
- medium HepG2

3.6.2 *Methods*

Table 1: Different hydrogels tested on rheometer

GEL Vol %	ELR Vol %
100	0
75	25
50	50
25	75
0	100

First of all, five hydrogels of each type were prepared in a 14 mm mold (volume 550 µL) as detailed in Section 3.3. The different types of hydrogels tested are shown on Table 1. The 14 mm diameter mould was used to guarantee that the area of the hydrogel was at least equal to or greater than the area of the parallel plate geometry. The exact volumes of reagents used for the hydrogel synthesis are shown in Appendix C.

The hydrogels were prepared the day before the measurements and kept in HepG2 medium for 24 h at 37 °C for reaching swelling equilibrium.

Rheological measurements were performed using a shear strain mode with the parallel plate geometry (12 mm diameter). The temperature was maintained at 37 °C for the duration of the measurements. The gap between the plates was adjusted for each measure until the axial force was positive (compression force) and close to 0.1 N. The experimental procedure consisted of two different measures:

FREQUENCY SWEEP: the storage and loss moduli were measured as a function of frequency. The oscillation strain was kept constant at 0.3% since this was the limiting value for a linear behavior known from previous amplitude sweep tests. The frequency oscillated in the range of 0.1-10 Hz;

AMPLITUDE SWEEP: the storage and loss moduli were measured as a function of strain. The oscillation frequency was kept constant at 1 Hz and the strain oscillated in the range of 0.1-20%

3.7 HEPARIN RELEASE TEST

High heparin retention was one of the properties sought in this project as it is necessary for the final application in hepatic drug toxicity studies.

Indeed, as discussed in the Section 1.5, heparin is able to bind HGF via affinity interaction. Consequently, high heparin retention leads to high affinity for HGF, which in turn is required to stimulate cells towards a hepatic phenotype.

Initially, an attempt was made to determine heparin retention using a toluidine blue test adapted from [62]. However, the results of these tests were inconclusive, so we decided to move on to a more reliable test based on fluorescent heparin.

If with the first test we analysed all the different polymers ratios and compared the use of both VKV-N_3 and HBD6-N_3, with the second one this was not feasible due to the high price of fluorescent heparin. Therefore, compromises had to be made:

- test only pure GEL, pure ELR and the GEL-ELR 50/50 ratio
- use only HBD6-N_3 on ELR
- use a low amount of heparin

The consequences of this last assumption will be discussed in detail in the results section (Chapter 4).

NOTE Although no significant results were obtained with toluidine blue, I think it was a fundamental part of the project as it represents the essence of scientific research. Not obtaining results is part of the journey and is nevertheless a positive result because it allows us to think about why the method did not work.

3.7.1 *Heparin release: fluorescence method*

Fluorescence is a technique for detecting particular components of complex biomolecular systems with extraordinary sensitivity and selectivity. Certain molecules, called fluorophores or fluorescent dyes,

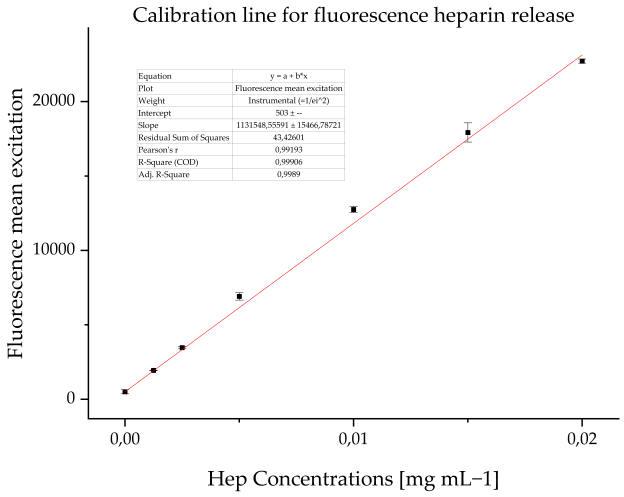

Figure 14: Calibration curve for heparin release in a solution based on emission at 535 nm.

are able to absorb and emit photons when excited at a specific wavelength and the emission results in their fluorescence. For what regards heparin, the absorption peak according to manufacturing data is set at 496 ± 5 nm, while the fluorescence peak at 515 ± 5 nm [63].

3.7.1.1 *Materials*

- heparin, Fluorescent Conjugate, from Thermo Fisher Scientific (USA)
- milliQ water
- sodium azide

3.7.1.2 *Methods*

CALIBRATION CURVE Firstly, a calibration curve was prepared using different dilutions of fluorescent heparin in a 0.1 molar solution of sodium azide (NaN_3) in Milli-Q water. Sodium azide was used as a preservative for the phosphate buffer and three replicates were prepared for each concentration. The calibration curve is shown in Figure 14.

The amounts of reagents and the calculations performed are reported in the appendix. The results output by the spectophotometer are listed in Table 2

INCORPORATION OF HEPARIN INTO THE HYDROGEL In order to quantify the heparin release, five different hydrogels of pure GEL, pure ELR and GEL-ELR 50/50 were prepared according to protocols described in Section 3.3. Each hydrogel had a volume of 200 µL and was

Table 2: Fluorescence excitation of heparin solution at different concentrations

Hep Conc [mg mL^{-1}]	Mean fluorescence
0.02	22720
0.015	17926
0.01	12749
0.005	6914
0.0025	3470
0.00125	1940
0	503

prepared on a mold of 8 mm. Fluorescent heparin was dissolved in milliQ water with a concentration of 8 mg mL^{-1} and kept overnight at 4 °C. For pure GEL hydrogels, heparin solution was added to GEL solution 30 minutes prior to hydrogel synthesis. For pure ELR, it was added to HBD6-N_3 30 minutes prior to hydrogel synthesis. For GEL-ELR hydrogels, heparin solution was added to HBD6-N_3 in the same procedure used for the pure ELR hydrogels. The final concentration of fluorescent heparin on each hydrogel was 0.1 mg mL^{-1}.

As control groups, 5 hydrogels of each type of 200 µL were prepared without incorporation of fluorescent heparin.

The exact volumes of reagents used for the hydrogel synthesis and the calculations made for obtaining these values are shown in Appendix D.

Table 3: Supernatant collection time for the heparin release test

Collection	time [h]
1	0
2	2
3	4
4	24
5	48
6	168 (7 day)

SUPERNATANTS COLLECTION After hydrogel synthesis, the hydrogels were immersed in 1 mL of milli-Q water with azide salt and kept at 37 °C. The supernatant was collected at six different time instants shown in Table 3 placed in 1.5 mL eppendorfs, and frozen at -80 °C. Each time the supernatant was collected, it was replaced with a fresh one.

SPECTOPHOTOMETRY Once all the supernatants at different time frames were collected, 100 µL of of each supernatant were put on a plate and the fluorescence was measured. The cumulative mass of heparin released could be obtained from these measurements by following the calculations reported in Appendix D.

3.8 HGF RELEASE TEST

3.8.0.1 *Materials*

- fluorophore DyLight 488 NHS Ester
- HGF-488
- Dimethylformamide (DMF), Scharlab (Spain),
- Slide-A-L dialysis device, Slide-A-Lyzer MINI (10000 MWCO)
- heparin sodium salt from porcine intestinal mucosa (Grade I-A, > 180 USP 1/g);

3.8.0.2 *Methods*

HGF release from hydrogels was quantified using fluorescent labelled HGF-488 molecules.

Due to the high price of HGF, the release was only tested for GEL-ELR 50/50 and two different assays were performed: the first compared hydrogels with heparin and HGF with a negative control of hydrogels with heparin but without HGF incorporation. The negative control was tested to assess a possible interaction of heparin with HGF fluency.

A second test was conducted on hydrogels with HGF but without heparin in order to assess the impact of heparin on HGF retention. Hydrogels without heparin or HGF were used as a negative control.

FLORESCENCE LABELLING OF HGF The aim of this procedure was to label HGF with the fluorophore DyLight 488 in order to identify HGF molecules by fluoroscopy analysis.

Initially, 50 µg of the fluorophore DyLight 488 NHS Ester were dissolved in 50 µL of DMF to obtain a solution at a concentration of 1 $mg\,mL^{-1}$. This solution will be referred to as solution A.

Subsequently, 10 µg molecules of HGF were dissolved in 100 µL of Phosphate-Buffered Saline (PBS) to obtain a 0.1 $mg\,mL^{-1}$ concentration. This solution will be referred to as solution B.

A dialysis of this solution (solution B) was then carried out in 0.05 M borax at pH 8.5 using a Slide-A-L dialysis device MINI (10000 MWCO), thus obtaining a 100 $mg\,mL^{-1}$ solution of HGF in Borax (solution C). The membrane was first hydrated in milliQ water for 10 minutes.

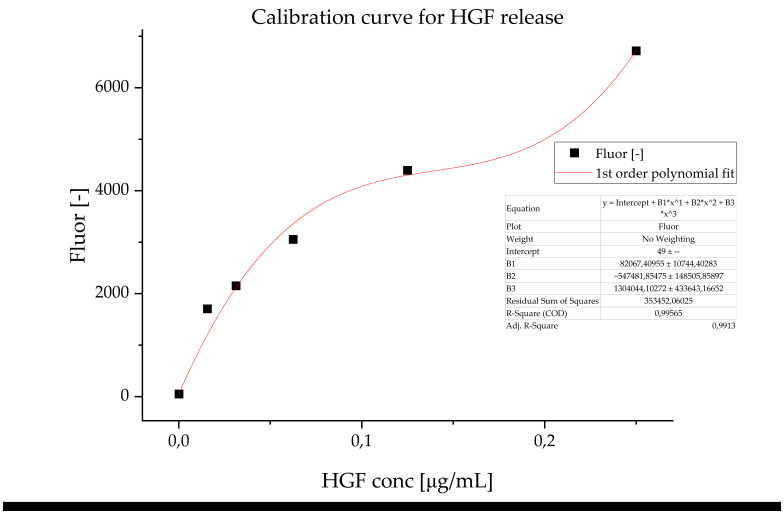

Figure 15: Calibration curve for HGF release for hydrogels with heparin

It was then necessary to calculate the volume $V_{DyLight488}$ of the solution containing the fluorophore (solution A) to be added to the HGF solution (solution C) in order to obtain labelled HGF (solution D). The formula used for this calculation was given by the provider of fluorophore DyLight 48 and is reported on Equation 3.8.0.2.

$$V_{DyLight488} = \frac{m_{HGF} \cdot 10 \cdot MW_{DyLight488}}{MW_{HGF} \cdot [C]_{DyLight488}} = 1.3\mu L \tag{6}$$

where:

m_{HGF}	0.01 mg
$MW_{DyLight488}$	1011 Da
MW_{HGF}	80000 Da
$[C]_{DyLight488}$	1 mg mL^{-1}

Therefore, 1.3 µL of solution A (fluorophore in DMF) was added to solution C. The mixture was left to react at RT for 1 h, protecting it from light.

Subsequently, solution D was dialysed in PBS 1X (-/-) using the same type of membrane as mentioned above and changing the PBS every hour for a total of 4 times.

This step involved exchanging the borax buffer with PBS, finally obtaining the desired solution (solution E) of HGF-labelled in PBS, which was then frozen at -20 °C for storage.

CALIBRATION CURVE First of all, a calibration curve was prepared with different dilutions of HGF-488 concentration in a solution of PBS. The concentration used and the calculations made are reported in Appendix E. Three 100 µL replicates of each concentration were prepared and their fluorescence measured at 488 nm using a spectropho-

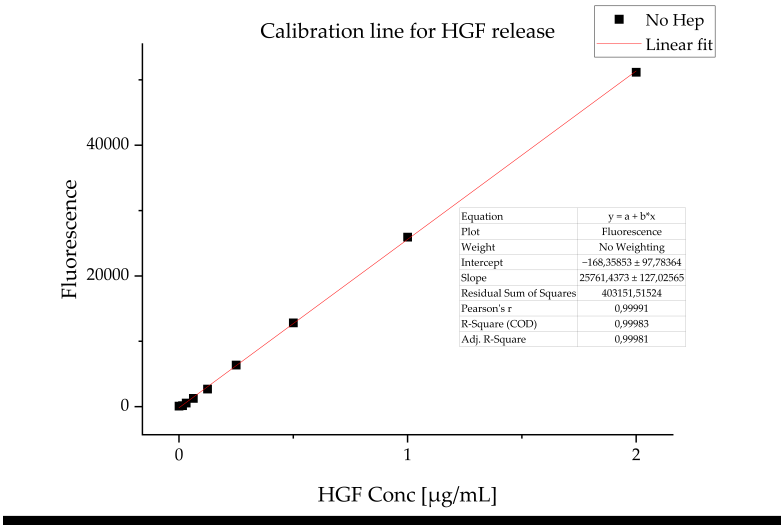

Figure 16: Calibration curve for HGF release for hydrogels without heparin

tometer. The fluorescence emission values at different concentration of HGF are reported on Table 4. The curve obtained (Figure 15) was interpolated with a third-degree polynomial, as the relationship between the concentration of HGF and fluorescence was not linear, especially at low concentrations. For this reason, it is necessary to perform further experiments by modifying the instrument parameters to obtain more reliable data at low concentrations of HGF.

For what regards the second assessment performed in order to test hydrogels without heparin, a new calibration curve (Figure 16) was prepared in the same modalities above mentioned with the value reported on Appendix E. This curve was interpolated with a line as the relation between HGF concentration and fluorescence was linear.

Table 4: HGF concentration prepared for calibration curves and relative fluorescence measured

HGF Conc [µg mL^{-1}]	Fluorescence hep	Fluorescence NO hep
2	35758	51169
1	19621	25932
0.5	10626	12831
0.25	6716	6380
0.125	4395	2709
0.0625	3054	1272
0.03125	2151	562
0.015625	1703	169
0	49	100.00

INCORPORATION OF HGF INTO THE HYDROGEL In order to measure the HGF release, five different hydrogels of GEL-ELR 50/50 were prepared according to protocols described in Section 3.3. Each hydrogel had a volume of 50 µL and was prepared directly on a plate.

Heparin was dissolved in DMEM with a concentration of 20 mg mL^{-1} and kept for 30 minutes at 4 °C.

For what regards the first assay, heparin solution was added to HBD6-N_3 solution and the solution obtained was kept for 30 minutes at 4 °C. In the second test performed, this step was not performed to assess the influence of heparin on HGF release.

Then, HGF solution was added to HBD6-N_3/(Hep) solution waiting 30 minutes for allowing homogenisation.

The final concentration of heparin on each hydrogel was 0.1 mg mL^{-1} while the final concentration of HGF on each hydrogel was 0.01 mg mL^{-1}.

As control groups, 5 hydrogels of 50 µL were prepared with incorporation of heparin but without HGF. Moreover, 3 hydrogels of 50 µL were prepared in the same condition without incorporation of HGF or heparin.

The exact volumes and calculations are reported in Appendix C

SUPERNATANTS COLLECTION After hydrogel synthesis, the hydrogels were immersed in 400 µL of PBS and kept at 37 °C. The supernatant was collected at six different time instants (0 h, 2 h, 4 h, 24 h, 48 h, 7 d), placed in 1.5 mL eppendorf tubes, and frozen at -80 °C. Each time the supernatant was collected, it was replaced with a fresh one.

SPECTOPHOTOMETRY Once that all the supernatants at different time frames were collected, 100 µL of each supernatant was put on a plate, ready for the measurements of fluorescence at 488 nm wavelength. For each supernatant the measure was repeated three time, using in this way 300 µL of each one. Finally, using the calibration line, the concentration of HGF was calculated and then the mass of HGF released according to the calculations reported on Appendix E,

3.9 STATISTICAL ANALYSIS

All the data were statistically analyzed by Tukey multiple comparison tests and ANOVA test trough *ORIGIN Pro* software (version 2022b). Statistical significance was accepted at $p<0.05$. Experimental results are expressed as the mean value (μ) $\pm$ standard deviation (σ).

4

RESULTS

This chapter presents the results obtained for the various experiments performed. The results refer to the different types of hydrogels tested (GEL-ELR 100/0, 75/25, 50/50, 25/75, 0/100), however, as described in Chapter 3, for economic reasons in some experiments only specific ratios were tested.

The statistical significance of the difference between the types of hydrogels was set at $\alpha = 0.05$ and *ANOVA* or *t-tests* were performed to asses the statistical difference between groups.

4.1 TYRAMINE INSERTION DEGREE

The degree of tyramine substitution in GEL-TYR was an important parameter to quantify as it is profoundly linked to the gelling capacity of hydrogels. As described in Section 1.3, the insertion of tyramine brings phenolic groups into the GEL chains, which are necessary for the reaction with H_2O_2 and HRP in order to form the hydrogel. If the degree of substitution of tyramine is too low, it means that only a few phenolic groups have been introduced, so the cross-linking may be too weak and the hydrogel may not form.

The degree of substitution was calculated for each batch of GEL-TYR according to the steps described in Appendix A. The mean value for the different bathes obtained during the project was 23.91, which is in line with the value 24 obtained by Poveda-Reyes et al. for the same procedures [64].

It can be concluded that no major errors were made during the GEL-TYR synthesis.

Furthermore, as the importance of the degree of tyramine insertion is related to the possibility of forming hydrogels, each batch was tested for the formation of a pure GEL hydrogel of 200 µL and gelation took place in all batches in approximately 10 minutes at RT.

According to these results, GEL could be utilized in order to obtain in situ gelling hydrogel.

4.2 RHEOLOGICAL MEASUREMENTS

Figure 17 shows the dependence of the storage modulus at different frequencies for VKV-N_3 and HBD6-N_3-based hydrogels with different polymer ratios.

Figure 18 represents the dependence of the loss modulus at different frequencies for the same types of hydrogels. In all series, the loss

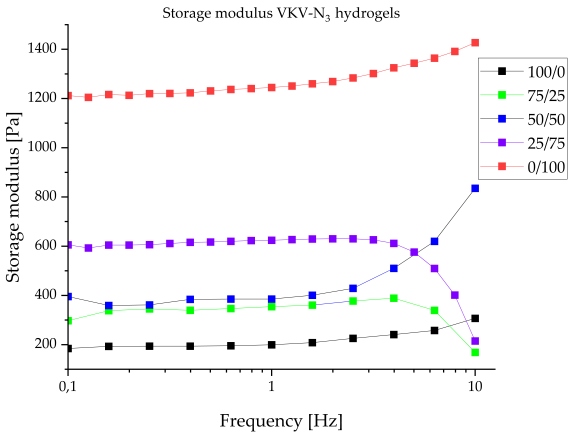

(a) VKV-N_3

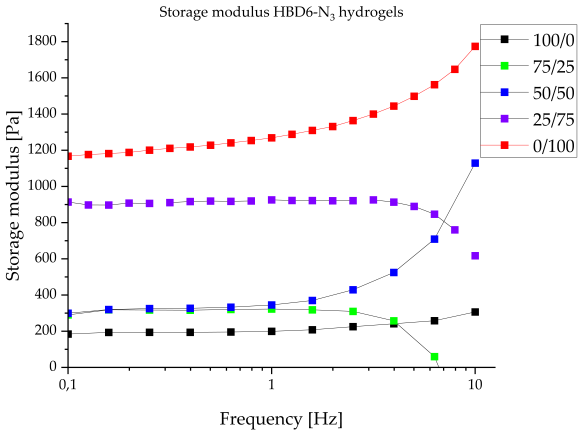

(b) HBD6-N_3

Figure 17: Storage modulus for hydrogels series at 1 Hz

modulus values were almost an order of magnitude lower than the storage modulus.

Finally, Figure 19 shows the dependence of the complex modulus at different oscillation strain for VKV-N_3 and HBD6-N_3 based hydrogels at different polymer ratios. In this graph, the linearity of the modulus for the deformation of 0.3 % set for the frequency range can be seen. At higher strains, a decrease in mechanical properties is noted.

Figure 20 reports the storage modulus at 0.3% of oscillation strain and 1 Hz of frequency for hydrogel of different ratios and composition. The numerical values are reported also in Table 5.

Pure GEL hydrogels present a storage modulus of 171.54 $\pm$ 20.05 Pa. Moulisová et al. [65] reported an storage modulus of 172 $\pm$ 38 Pa for 2% w/v hydrogels with the same crosslinking mechanism. It was expected that working with a higher polymer concentration the modulus would be higher, but a possible explanation could be the

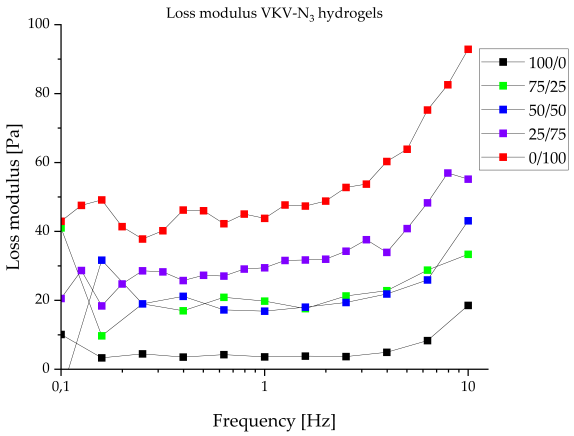

(a) VKV-N_3

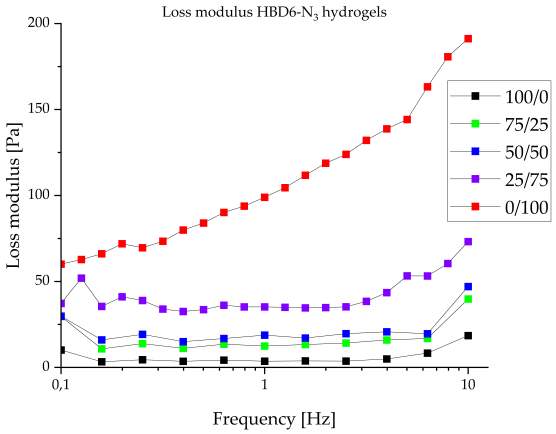

(b) HBD6-N_3

Figure 18: Loss modulus for hydrogel series at 1 Hz

different protocol used. In our project, the hydrogels were immersed in medium for 24 h, while Moulisová et al. performed in-situ measurements.

By increasing the volume percentage of ELR to GEL-ELR 75/25, an increase in mechanical properties was observed and there was no statistical difference between the VKV-N_3-based ELRs and the HBD6-N_3-based hydrogels.

The storage modulus for the ratio GEL-ELR 50/50 was 384 $\pm$ 93 Pa for VKV-N_3 and 337 $\pm$ 67 Pa for HBD6-N_3 hydrogels, that is in range with the value reported by Georges et al. on rat livers ($G^{'}$ around 400 Pa for healthy animals [66]). On the other hand, Ozeki and Tabata reported a slightly higher value of the storage modulus for the human liver, about 1 kPa [38].

Nevertheless, the values reported in the literature indicate a range of a few hundred Pa and therefore it can be concluded that the

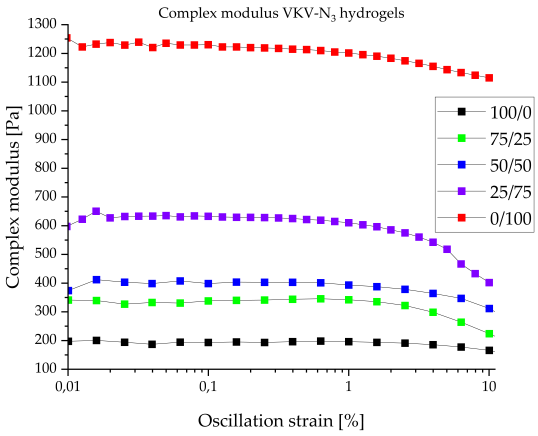

(a) VKV-N_3

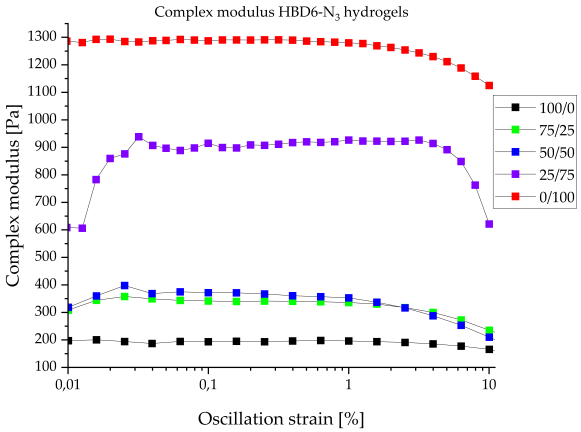

(b) HBD6-N_3

Figure 19: Complex modulus for hydrogel series at 1 Hz

GEL-ELR 50/50 ratio is suitable for liver tissue engineering applications.

By increasing the ratio of ELR to GEL-ELR 25/75, there was an increase in the storage modulus in both VKV-N_3 and HBD6-N_3 hydrogels. ELR. The HBD6-N_3 hydrogels presented a slightly higher modulus, but there was no statistically significant difference between the two ELR.

As for the pure ELR hydrogels, they presented the highest values of storage modulus: VKV-N_3 (1245 $\pm$ 199 Pa) and HBD6-N_3 (1034 $\pm$ 332 Pa). In this case, HBD6-N_3 presented a slightly lower modulus, but there was no statistically significant difference between the two ELR. As can be seen, the standard deviation is rather high; further experiments will be performed by testing more hydrogels.

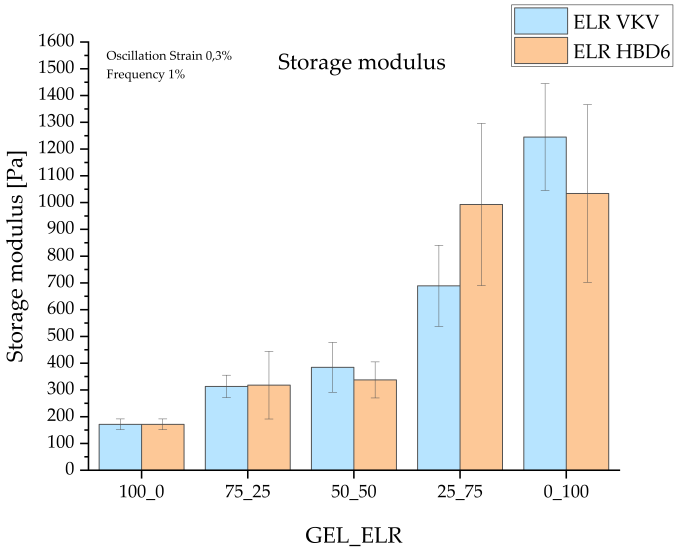

Figure 20: Storage modulus for different hydrogels

Table 5: Storage modulus for different hydrogels

GEL/ELR	VKV G_S [Pa]	HBD6 G_S [Pa]
100/0	171 ± 20	
75/25	313 ± 41	317 ± 126
50/50	384 ± 93	337 ± 67
25/75	688 ± 151	992 ± 302
0/100	1245 ± 199	1034 ± 332

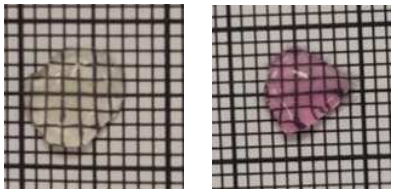

(a) fresh weight (b) wet weight

(c) dry weight

Figure 21: EWC: pure GEL hydrogels at different stages

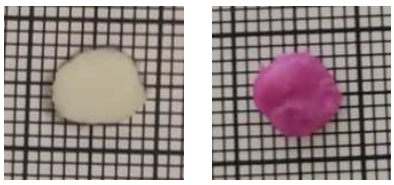

(a) fresh weight (b) wet weight

(c) dry weight

Figure 22: EWC: pure ELR hydrogels at different stages (HBD6-N_3)

4.3 SWELLING BEHAVIOUR

Two different comparisons were done: first of all it was compared the EWC of pure GEL hydrogels (Figure 21), pure ELR hydrogels (Figure 22) and GEL-ELR 50/50 hydrogels (Figure 23. In this assay, ELR was formed only with HBD6-N_3. Then, pure ELR hydrogels produced with VKV-N_3 and HBD6-N_3 were compared to asses the difference between the ELR azides used.

PURE GEL, PURE ELR AND GEL-ELR 50/50 The mean values and standard deviation of each type of hydrogel are given in Table 7, while a graphical representation of these values is provided in Figure 24. The pure GEL hydrogel presented the highest EWC (17.58), while the the 50/50 blend and pure ELR had lower values of 5.07 and 3.32, respectively. The value of the mixture is reasonable in that it is

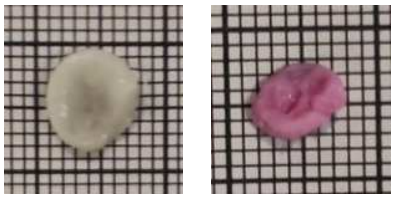

(a) fresh weight (b) wet weight

(c) dry weight

Figure 23: EWC: GEL-ELR 50/50 hydrogels at different stages

between the two values of the pures, since the properties are a combination of those of the pures. However, it was closer to the pure ELR and there was no statistical difference between the two considering a significance $\alpha = 0.05$. On the other hand, there was a statistical difference between the pure GEL hydrogels and both the pure ELR and the 50/50 mixture with p-values less than 0.001.

In [64], the authors worked with 2 % (w/v) gel hydrogels and obtained an EWC value of 29.24 ± 1.69, whereas [30] reported a value of 33.66 ± 6.35 for the same type of hydrogel.

In our project, we worked with hydrogels at 8 % (w/v) and this explains the lower value of EWC obtained for pure hydrogels GEL, as more concentrated hydrogels are expected to be less porous with a lower water-holding capacity [30].

According to these results, GEL hydrogels are able to retain more water than ELR hydrogels, and this is related to the different microscopic structure. In pure GEL hydrogels, a more porous structure with higher porosity is expected.

VKV-N_3 AND HBD6-N_3 In Table 7, the mean values of EWC for VKV-N_3 and HBD6-N_3 are reported numerically. VKV-N_3 hydrogels presented a lower EWC of 1.86, while HBD6-N_3 based hydrogels presented an almost double value of 3.42. A t-test was performed to determine whether there was a significant difference between VKV-N_3 and HBD-N_3 EWC values and the significance of the test was set at p=0.005. The p value was found to be p=0.0013, indicating a statistical difference between the two groups (Figure 25).

Table 6: Descriptive statistics of EWC for different types of hydrogels

Hydrogel type	Mean EWC ± std
GEL_ELR_100_0	17.59 ± 0.72
GEL_ELR_50_50	5.07 ± 1.36
GEL_ELR_0_100	3.33 ± 0.74

Table 7: Descriptive statistics of EWC for pure ELR hydrogels

ELR-N_3	Mean EWC [-]	Std
VKV	1.86	0.46
HDB6	3.42	0.96

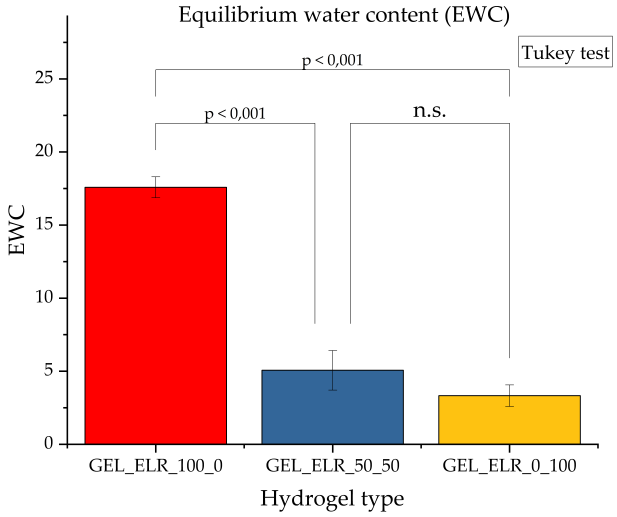

Figure 24: EWC comparison for different types of hydrogels

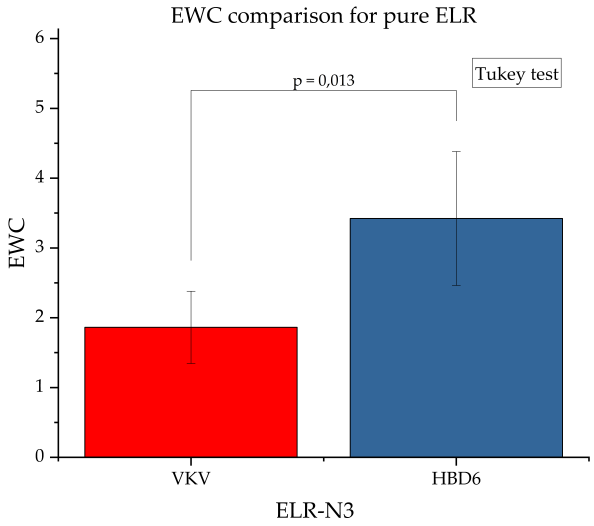

Figure 25: EWC comparison between HBD6-N_3 and vkv-N_3 pure ELR based hydrogels

4.4 MICROSCOPICAL ANALYSES

The morphology, microscopic structure and pore sizes of the different hydrogels were studied by FESEM. This instrument allows a detailed image of the sample surface to be obtained by scanning with a highly focused beam of high and low energy electrons [60].

Three different hydrogels were compared: pure GEL, pure ELR and GEL-ELR 50/50 ratio. The microscopic structure with a magnitude of 500x is shown in Figure 26, while Figure 27 shows the structure with a greater magnitude of 2000x.

All the hydrogels presented an interconnected honeycomb-like porous structure, typical of natural origin hydrogels [64]. Additionally, no evident phase separation was observed in the mixed GEL-ELR hydrogels, suggesting satisfactory homogeneity. Table 8 shows the pore area and the relative EWC previously calculated. Pure GEL had the highest pore area (31.14 μm^2) and the highest EWC (17.59), which was reasonable as the pore size is proportional to the water content that can be retained in the hydrogel. The results obtained for the mixture and the pure ELR were also consistent: a smaller pore size corresponded to a smaller EWC. GEL-ELR 50/50 presents a pore area of 17.06 μm^2 and EWC of 5.07, while pure ELR an area of 12.62 μm^2 and a EWC of 3.33. However, it must be noticed that the standard deviation of the pore area were very elevated values and that is due to the low precision of the software used for the analysis of imaging (ImageJ).

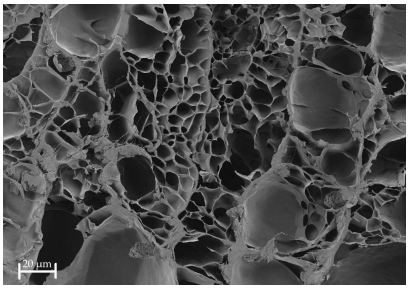

(a) pure GEL

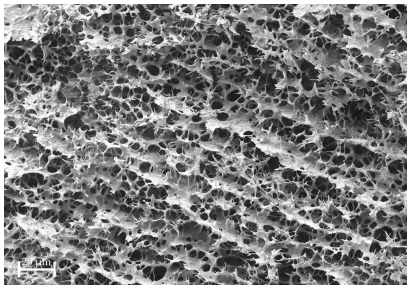

(b) GEL-ELR

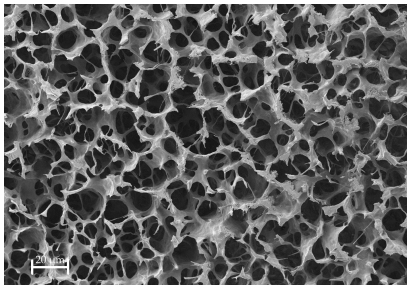

(c) pure ELR

Figure 26: Comparison of microscopy of various hydrogel types at 500X magnification

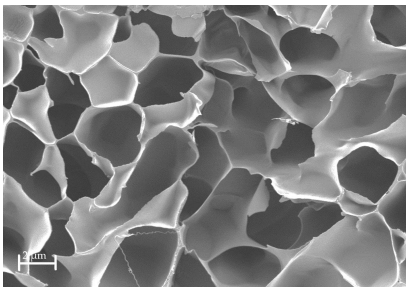

(a) pure GEL

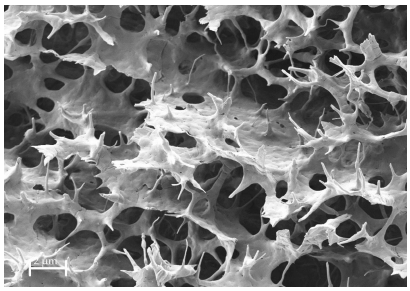

(b) GEL-ELR

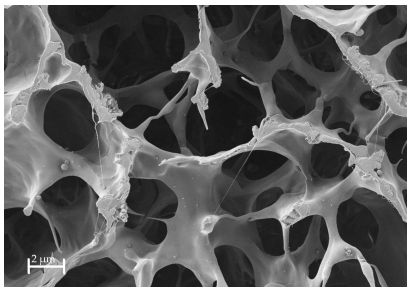

(c) pure ELR

Figure 27: Comparison of microscopy of various hydrogel types at 2000 X magnification

Table 8: Pore areas for different types of hydrogels

GEL/ELR	AREA(μm^2)	EWC
100/0	31.14 ± 2.95	17.59 ± 0.72
50/50	17.06 ± 4.64	5.07 ± 1.36
0/100	12.62 ± 2.95	3.33 ± 0.74

4.5 HEPARIN RELEASE

Quantification of heparin release was performed by two different techniques, as discussed in Section 3.7.

4.5.1 *Toluidine blue*

All the different ratios were analyzed by the toluidine blue method, but no significant results were obtained. The immediate conclusion was that another technique needed to be found. One possible explanation could be the interference of hydrogel particles released into the supernatant, which caused higher absorbance values and did not allow differences to be seen between the test and control groups.

4.5.2 *Fluorescence*

ASSUMPTION AND CONSEQUENCES Due to the high cost of fluorescent heparin, compromises had to be made:

- test only pure GEL, pure ELR and the GEL-ELR 50/50 ratio;
- use only HBD6-N_3 on ELR;
- use a low amount of heparin.

We decided to utilize only HBD6-N_3 because of the heparin-binding domain present in its structure, which should give increased heparin retention. State the efficacy of using HBD6-N_3 instead of VKV-N_3 would require a comparison of hydrogels, but for economic reasons this has not yet been done.

The third consequence also had an important impact on the analysis: since the active sequence of HBD6-N_3 is present 6 times per molecule, theoretically each molecule could bind to 6 molecules of heparin. Therefore, to occupy all HBD6-N_3 sites, the total number of moles of heparin would have to be six times the total moles of HBD6-N_3. Since the Molar Weight (MW) of heparin is 12000 $g\,mol^{-1}$ and the MW of HBD6-N_3 is 60000 $g\,mol^{-1}$, the mass ratio Hep-HBD6-N_3 would be 1.2. The assay was performed with hydrogel with a volume of 200 µL, that is, with 50 µL of HBD6-N_3 solution at 8%

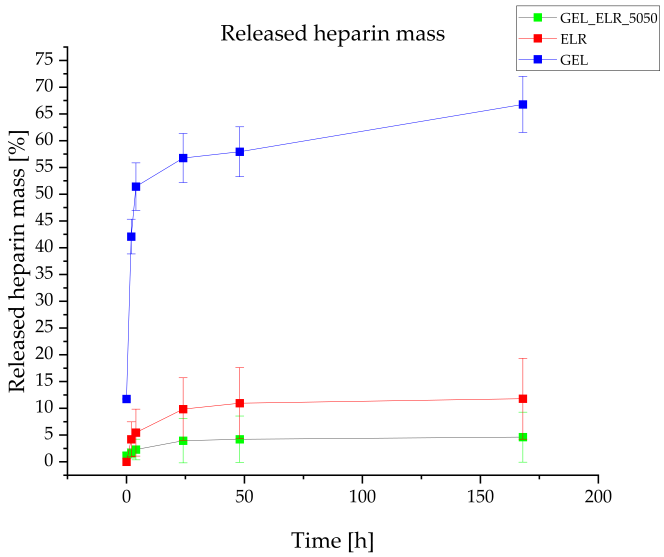

Figure 28: Cumulative release of heparin over time using the fluorescence method

concentration. This means that the mass of HBD6-N_3 was 4 mg per hydrogel and the mass of heparin should be 4.8 mg. According to the commercial cost of 415 €/mg, per hydrogel there would be a cost of 1992 €just for fluorescent heparin. Considering more hydrogels, this was financially unsustainable. Therefore, we set a lower amount of heparin of 0.02 mg per hydrogel, but in this case less than 0.01% of the HBD6-N_3 molecules bound to heparin. As a consequence, by reducing the amount of ELR in the mixture, the retained mass did not change because the amount of HBD6-N_3 present was sufficient to bind heparin.

Table 9: Percentage of total heparin mass retained for different types of hydrogels

GEL/ELR	Hep mass retained [%]
100/0	33 ± 5
50/50	95 ± 5
0/100	88 ± 8

CUMULATIVE RELEASE As presented in Section 3.7, the heparin released mass was evaluated in 6 different time intervals: t=0,2,4,24,48,168 h.

Figure 28 shows the cumulative heparin released expressed as a percentage of total mass and compares pure GEL, pure ELR and 50/50 blend. Figure 29 compares the final heparin retention for the three

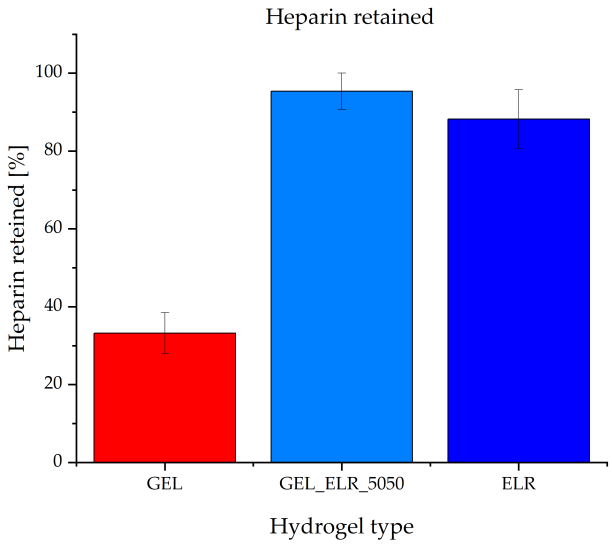

Figure 29: Retention of heparin after 7 days using the fluorescence method

types of hydrogels, and these values were obtained as the difference between 100% and the mass liberated. Talking about low heparin release or high retention is irrelevant, hence these terms will be interchanged in the following discussion.

The pure ELR hydrogels and GEL-ELR 50/50 had the highest heparin retention after 7 days and this can be imputed to the presence of the heparin-binding domain in the HBD6-N_3 molecules. There was no statistical difference between pure ELR and GEL-ELR 50/50 mixture: as explained above, this is a consequence of the low amount of heparin incorporated into the hydrogels. Using the calculated theoretical amount of heparin, the 50/50 blend is expected to maintain an intermediate amount of heparin.

As the retained heparin for ELR hydrogels was approximately 90%, this result confirmed our hypothesis of increasing heparin retention with the use of HBD6-N_3 ELR. Having demonstrated the retention of heparin, it was possible to proceed with the retention test of HGF. There was a statistical difference between hydrogels with ELR and pure GEL hydrogels, that present a release of 67%. Although lower, GEL hydrogels also retained a small amount of heparin; one possible explanation could be the electrostatic interaction between heparin and gelatin chains. Indeed, at physiological pH, type A gelatin is positively charged, whereas heparin molecules are highly negatively charged due to their sulphate residues. [67].

Table 10: Percentage of HGF mass released for different types of hydrogels

Time [h]	Released HGF mass %	
	NO HEP	HEP
0	4 ± 1%	2% ± 1%
2	13 ± 2%	20% ± 4%
4	19 ± 2%	22% ± 4%
24	22 ± 3%	22% ± 4%
48	24 ± 3%	23% ± 4%
168	26 ± 3%	24% ± 4%

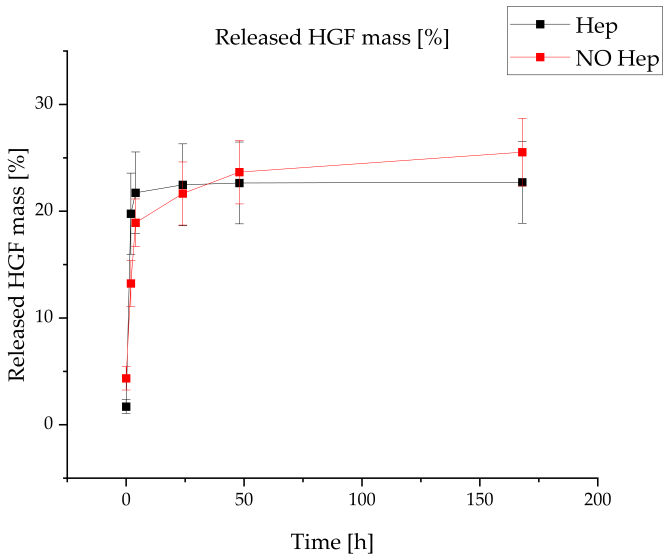

Figure 30: Comparison of HGF release mass for GEL/ELR 50/50 hydrogels with or without heparin incorporation

4.6 HGF RELEASE

As presented in Section 3.8, the HGF released mass was evaluated in 6 different time intervals: t=0,2,4,24,48,168 h. Figure 30 shows the cumulative HGF released expressed as a percentage of total HGF incorporated mass and compares GEL-ELR 50/50 synthesised with or without heparin. The numerical values are also given in Table 10.

It was expected that there would be a greater difference between the two systems, as heparin should attract HGF and consequently the release should be lower. In contrast, there was no significant difference in the release by including heparin in the hydrogels. One possible explanation could be the high size of the HGF, which have a MW of about 80000 Da and could stay entrapped in the chains regardless of the presence of heparin.

However, it can be seen that the curve of the hydrogels without heparin did not reach the plateau region and therefore there could be a higher release of HGF at longer times. This means that this experiment should be repeated to examine the release over a longer time interval, e.g. considering 14 days.

Moreover, further tests will also be needed on pure GEL and pure ELR hydrogels to evaluate the importance of heparin in increasing HGF retention.

Part III

FINANCIAL ANALYSIS

5 BUDGET

This chapter illustrates the calculation performed to obtain the project budget in order to study its economic feasibility.

The necessary budget was calculated by conceptually categorising the expenses into four different categories: Table 11 reports the net salaries of the employees, including the student, the tutor and the supervisor. It should be noted that the student did not receive any financial salary during the project, but in order to provide as accurate an estimate of the final cost as possible, his workload must be taken into account. Next, Table 12 shows the net costs of the laboratory instruments used during the project. Then, Table 13 shows the gross costs of the reagents needed to perform the various syntheses and analyses during the project. Finally, Table 14 shows the hourly costs of the instruments used.

Table 11: Budget for professional workers

N.°	Unit	Description	Unit price [€]	Quantity	Total [€]
1	h	Student	12	300	3600
2	h	Tutor/a	45	300	13500
3	h	Cotutor/a	45	45	2025
				Total price	19125

Table 12: Project budget for lab equipment

Nº	Unit	Description	Unit price [€]	Quantity	Total [€]
1	ud	Lab coat	22.5	1	22.5
2	ud	Latex glove box	5.95	4	23.8
3	ud	Protective glasses	8.95	1	8.95
4	ud	Gas mask	30.5	1	30.5
5	ud	Particle mask	7.25	1	7.25
6	L	mQ water	0.2	8	1.6
7	L	Distilled water	0.2	150	30
8	L	Absolute ethanol	3.93	0.5	1.965
9	m	Dialysis membrane	3.2	0.15	0.48
10	ud	Laboratory Tweezers	8.73	1	8.73
11	ud	Metal spatula	3.66	1	3.66
12	ud	Measuring cylinder 10 mL	2.35	1	2.35
13	ud	Beaker 3 L	4.62	1	4.62
14	ud	25 mL beaker	3.56	1	3.56
15	ud	Pyrex flasks 80 mL	6.74	2	13.48
16	ud	150 mL urine containers	0.19	25	4.75
17	ud	1000 µL micropipette	215	1	215
18	ud	200 µL micropipette	215	1	215
19	ud	20 µL micropipette	215	1	215
20	ud	1000 µL micropipette tip box	65.25	3	195.75
21	ud	200 µL micropipette tip box	39.16	3	117.48
22	ud	20 µL micropipette tip box	60.2	3	180.6
23	ud	Eppendorf 0.5mL	0.05	200	10
24	ud	Eppendorf 1.5mL	0.07	400	28
25	ud	P48 Deep Well Plates	2.81	10	28.1
				Total cost	**1373.125**

Table 13: Project budget for reagents

Nº	Unit	Description	Unit price [€]	Quantity	Total [€]
1	g	Gelatin (Type A)	0.475	10	4.75
2	L	DMEM medium	35.58	0.1	3.558
3	g	EDC	62.3	1.42	88.466
4	g	MES	2.82	7.08	19.9656
5	g	NHS	3.84	0.05	0.192
6	g	Sodium chloride (NaCl)	0.15	400	60
7	g	Tyramine Hydrochloride	15.1	1.2	18.12
8	L	Hydrogen peroxide (H_2O_2)	7.17	0.02	0.1434
9	L	Peroxidase (HRP)	38.6	0.02	0.772
10	ud	Liver growth factor (HGF)	170	0.4	68
11	ud	Heparin. Fluorescein Conjugate	395	1	395
12	ud	Fluorescent marker (DyLight 488 NHS Ester Kit)	249	0.2	49.8
13	ud	Borate buffer packets	4.625	1	4.625
14	L	N.N-Dimethylformamide (DMF)	5.21	0.00005	0.000261
				Total cost	**713.3923**

Table 14: Project budget for instruments

Nº	Unit	Description	Unit price [€]	Quantity	Total [€]
1	h	pH meter	0.3	9.5	2.85
2	h	Stove 37ºC	0.1	168	16.8
3	h	Precision scale	0.15	9.5	1.425
4	h	Spectrophotometer	0.8	14	11.2
5	h	Rheometer	10	18	180
6	h	desiccator	0.1	192	19.2
7	h	Fluorescence reader (NanoDrop)	2.25	1.5	3.375
8	h	Fluorescence plate reader (Victor)	1.42	2	2.84
9	h	Magnetic stirrer	0.2	525	105
10	h	FSEM	25	3	75
10	h	Lyophilizer	9.46	672	6357.12
				Total cost	**6**774.81

Final budget

Table 15: Total gross cost for hydrogels synthesis

Description	Total cost [€]
Lab equipment	170
mQ water	1.6
Distilled water	30
Absolute ethanol	1.965
Gelatin (A)	4.75
DMEM medium	3.558
EDC	88.466
MES	19.9656
NHS	0.192
Tyramine Hydrochloride (Tyr-HCl)	18.12
Hydrogen peroxide (H202)	0.1434
Peroxidase (HRP)	0.772
Borate buffer packets	4.625
Dialysis membrane (12.4k MWCO)	0.48
Laboratory Tweezers	8.73
150 mL urine containers	4.75
pH meter	2.85
Stove 37°C	16.8
Precision scale	1.425
Spectrophotometer	11.20
Rheometer	180
desiccator	19.20
Magnetic stirrer	105
Lyophilizer	5871.24
Total	**6486.20**

The final cost was calculated as the sum of reagents, laboratory instruments and personnel. Table 16 shows the gross total material cost, including reagents, laboratory instruments and equipment. This cost was calculated by allocating the cost of each chapter and it can be seen that the highest is attributed to hydrogel synthesis. Each cost was determined by considering the individual cost of each reagent/tool listed above and the reagents/materials needed described in Chapter 2. Table 15 reports as a methodology example how the total hydrogel synthesis cost was calculated. This is the highest cost

and the most expensive task was the use of the lyophilizer, which accounted for almost 90% of the total cost. It should be noted that the synthesis of the hydrogel is closely related to the characterisation, as the hydrogel was synthesised mainly to perform experiments. However, as this part has more of a methodological purpose than an exact economic analysis, the costs were only classified according to the different sections of the Chapter 3. Once the total cost of materials was obtained, personal costs were added up and 13% of the subtotal was considered as general and administrative costs. This value was selected on the basis of the median of the reported general and administrative costs reported by [68].

The total cost without Value Added Tax (VAT) of the project was estimated at 16258 €

The total cost considering VAT was estimated at 19672 €.

Table 16: Total material cost

Task	Total cost [€]
Synthesis of Hydrogel	6486
Rheological characterization	197
EWC determination	48
Microscopy	95
Release of Hep	384
Release of HGF	278
Material cost	7488

Table 17: Final budget

Material cost	7488 €
Personal cost	6900 €
General and Administrative (13%)	1870 €
Total net cost	16258 €
IVA(21%)	3414 €
Total gross cost	**19672 €**

Part IV

CONCLUSION

6 CONCLUSION

The purpose of this work was demonstrate the potential of using a novel Gelatin-Elastin (GEL-ELR) based hydrogel as a platform for liver cells, with future applications for drug toxicity testing. The choice of combining these materials was based on the consideration that Gelatin (GEL), through its RGD domains, promotes cell attachment, while Elastin-Like Recombinamers (ELR), through their heparin binding sites, were expected to attract the HGF required for the development of the liver phenotype.

SWELLING BEHAVIOUR The swelling ability was compared trough EWC measured. Pure GEL hydrogels presented the highest value (17.59 ± 0.72), while GEL-ELR 50/50 (5.07 ± 1.36) and pure ELR (3.33 ± 0.74) had lower values. No statistical difference were found between GEL-ELR 50/50 and pure ELR. Pore sizes were consistent with these values: pure GEL presented the highest area (31.14 ± 2.95 μm^2), while GEL-ELR 50/50 (17.06 ± 4.64 μm^2) and pure ELR (12.62 ± 2.95 μm^2) had lower values.

MECHANICAL PROPERTIES The storage modulus (G') rose by almost an order of magnitude by increasing the content of ELR from pure GEL (172 ± 20) to pure ELR (1245 ± 200 Pa for VKV-N_3 and 1034 ± 332 Pa for HBD6-N_3).

The intermediate ratios presented storage modulus values between pure:

- GEL-ELR 75/25: 313 ± 20 Pa for VKV-N_3 and 318 ± 127 Pa for HBD6-N_3;
- GEL-ELR 50/50: 384 ± 42 Pa for VKV-N_3 and 338 ± 67 Pa for HBD6-N_3;
- GEL-ELR 25/75: 689 ± 152 Pa for VKV-N_3 and 993 ± 303 Pa for HBD6-N_3.

No statistical differences in the mechanical properties were noted between the VKV-N_3 and HBD6-N_3 hydrogels. This was reasonable as the structure of the two ELR is similar and the main difference only concerns the bioactive sequence for heparin binding in HBD6-N_3. As the standard deviation was relatively high, more hydrogels should be tested in order to determine more representative values.

The GEL-ELR 50/50 mixture had the most similar accumulation modulus to that of liver reported in the literature of a few hundred Pa.

Therefore, we focused on this mixture for further analysis. The use of equal proportions of GEL and ELR also allows the advantages of both materials to be exploited.

HEPARIN RETENTION Pure ELR hydrogels showed the highest heparin retention (96%), demonstrating that the use of HBD6-N_3 increased the ability of hydrogels to bind heparin. Pure GEL hydrogels showed lower values (33%). GEL-ELR 50/50 showed similar retention to pure ELR (89%), although a more expensive test would be needed to detect the differences.

HGF RETENTION The ability of hydrogels to attract HGF is critical to activate the cell signaling and simulate the hepatic phenotype. Because GEL-ELR 50/50 showed liver-like mechanical properties and high heparin-retention capacity, only this type of hydrogel was tested for HGF. Two different systems have been tested: GEL-ELR 50/50 with incorporation of heparin and GEL-ELR 50/50 without incorporation of heparin. The system with heparin showed a retention of HGF of 78 $\pm$ 3%, while in the system without heparin the retention was 74 % $\pm$ 3%. A greater difference between the two systems was expected, however, the high size of HGF might allow retention regardless of the presence of heparin. Further tests will also be needed on pure GEL and pure ELR to evaluate the importance of heparin in increasing HGF retention.

7 FUTURE RESEARCH

In this project, a series of hydrogels with 8% w/v ratios of GEL-ELR (GEL-ELR 100/0, 75/25, 50/50, 25/75, 0/100) were compared in terms of mechanical properties, EWC, microstructure, heparin retention, and HGF retention.

Due to the high cost of fluorescent heparin, it was not possible to evaluate the heparin retention of the whole series of hydrogels and it was decided to test only the main ratio of interest: GEL-ELR 50/50. On the other hand, it would also be interesting to test hydrogels made with VKV-N3 to evaluate the importance of the presence of the heparin-binding domain in the ELR chains in terms of heparin retention by the hydrogel.

A similar reasoning could also be made in terms of HGF retention, as only the GEL-ELR 50/50 with HBD6 was tested for economic reasons. Pure GEL and pure ELR were also tested for heparin release; it would be appropriate to test the same ratio for HGF release as well.

Another aspect that should be improved is the methodology of HGF release, as the relationship between HGF concentration and fluorescence was found to be nonlinear for low concentrations. Therefore, interpolation was performed with a third-degree polynomial, but this introduces interpolation errors since the relationship should be linear. Further tests should be performed with different instrument settings (excitation exposure time, excitation intensity, etc.) in order to obtain more reliable data.

Another possible task could be to analyze hydrogels as a function of temperature variation, for example by means of a Differential Scanning Calorimetry (DSC). Indeed, such a method would allow the identification of possible phase transitions.

Finally, studies with hepatocytes were not performed because time for this project was limited, but the next step will be encapsulate cells within the hydrogels and evaluate their viability and hepatic functionality.

3

Part V

APPENDIX

A

CALCULATIONS FOR GELATIN-TYRAMINE SYNTHESIS

The main objective of this appendix is to show the calculations done to calculate the proportions and mass of the different reactants in the synthesis of Gelatin-Tyramine (GEL-TYR). All the calculations refers to a single batch.

A.1 DEFINITION OF VARIABLES

Table 18 shows several quantities commonly used to describe the concentration of a solution.

Table 18: Definition of different type of concentrations

Type of concentration	UoM	Definition
Mass concentration (ρ_i)	$[g\,L^{-1}]$	mass of a constituent divided by the volume of the mixture
Molar concentration (c_i)	$[mol\,L^{-1}]$	moles of a constituent divided by the volume of the solution
Number concentration	$[L^{-1}]$	unit of constituent divided by the volume of the solution
Volume concentration (V_i)	$[L\,L^{-1}]$	Volume of a constituent divided by the volume of the solution

Multiplying the mass or molar concentration of a constituent by the volume of the solution (V_i) yields the mass (m_i) and moles (n_i) of that constituent, respectively.

$$m_i[g] = \rho_i[g\,L^{-1}] \cdot V[L] \tag{7}$$

Moreover, knowing the MW, is possible to convert the mass in grams of a reagent into moles, and vice versa.

$$\frac{mass[g]}{MW[g\,mol^{-1}]} = moles[mol] \tag{8}$$

Therefore, according to the fundamental principle of conservation of mass, between two solutions with the same amount of moles of solute i is always valid:

$$c_i[\text{mol L}^{-1}] \cdot V_i[\text{L}] = c_f[\text{mol L}^{-1}] \cdot V_f[\text{L}] \tag{9}$$

A.2 CALCULATIONS

Table 19: Molar weight of reagents used for hydrogel synthesis

Reagent	Molar weight
GEL	50-100 kDa
Tyramine (TYR)	173,64 g mol^{-1}
EDC	191,68 g mol^{-1}
NHS	115,09 g mol^{-1}

Table 20: molar ratio of reagents used for hydrogel synthesis

Reagents	Molar ratio
TYR: COOH	2:1
EDC: COOH	2:1
EDC:TYR	1:1
NHS: EDC	1:10

We want to have 20 mL of 2% w/v gelatin solution in 50 mM MES. Hence, the needed mass of gelatin is:

$$m_{GEL} = 20\text{mg mL}^{-1} = 400\text{mg} \tag{10}$$

Therefore, the needed mass of MES is :

$$m_{MES} = 50\text{mM} \cdot 20\text{mL} \cdot 195.24\text{g mol}^{-1} = 195.24\text{mg} \tag{11}$$

According to the manufacturer's data, there are 0.0008 mol of COOH groups each gram of GEL. Therefore, in 400 mg of GEL the number of moles of COOH groups is:

$$n_{COOH} = m_{GEL} \cdot 0.0008 = 10^{-4}\text{mol} \tag{12}$$

Using the molar ratio between tyramine and GEL shows in Table 20, the number of moles of tyramine and the needed mass of tyramine can be calculated as:

$$n_{TYR} : n_{COOH} = 2 : 1 \tag{13}$$

$$n_{TYR} = 2 \cdot n_{COOH} = 6.4 \cdot 10^{-4}\text{mol} \tag{14}$$

$$m_{TYR} = n_{TYR} \cdot MW_{TYR} = 111.13\text{mg} \tag{15}$$

Using the molar ratio between TYR and EDC shows in Table 20, the number of moles of EDC and the needed mass of EDC can be calculated as:

$$n_{TYR} : n_{EDC} = 1 : 1 \tag{16}$$

$$n_{EDC} = n_{COOH} = 6.4 \cdot 10^{-4} \text{mol} \tag{17}$$

$$m_{EDC} = n_{EDC} \cdot MW_{EDC} = 122.68 \text{mg} \tag{18}$$

Finally, using the molar ratio between NHS and EDC shows in Table 20, the number of moles of NHS and the needed mass of NHS can be calculated as:

$$n_{NHS} : n_{EDC} = 1 : 10 \tag{19}$$

$$n_{NHS} = 0.1 \cdot n_{COOH} = 6.4 \cdot 10^{-5} \text{mol} \tag{20}$$

$$m_{NHS} = n_{NHS} \cdot MW_{NHS} = 7.36 \text{mg} \tag{21}$$

B

CALCULATIONS OF THE DEGREE OF TYRAMINE SUBSTITUTION

The main objective of this appendix is to present the calculations done to calculate the degree of Tyramine Substitution on GEL-TYR hydrogels. This value is significant to determine because it is closely linked to the gelling of the hydrogels: a low value indicates an insufficient presence of tyramine inserts in the gelatin chains with the impossibility of crosslinking.

B.1 ABSORBANCE MEASUREMENT

Firstly, a solution of GEL-TYR was prepared in 1.5 mL of MilliQ water from each batch at a concentration of 0.1 % w/v, thus dissolving 1.5 mg of GEL-TYR in 1.5 mL of water. This solution was kept for about 1 hat 37 °C to allow dissolution. Subsequently, 450 µL of the solution were placed on a UV cube ready to be analysed with the spectrometer. From the spectrophotometer measurements, we obtained the absorbance (A) of GEL-TYR solution at different wavelengths. According to literature, the absorbance peak of TYR is set a $\lambda = 275$nm and this value was used for all the calulcations. This procedure was repeated three times for each batch, resulting in three different absorbance values.

B.2 CALCULATION OF THE DEGREE OF TYRAMINE SUBSTITUTION

The calibration curve (Figure 31 prepared as described in, shows that there is a linear relationship between the tyramine mass concentration (ρ_{TYR}) and the measured absorbance (A).

$$A = 4.1479 \cdot c_{TYR}[\text{mg mmol}^{-1}] \tag{22}$$

Knowing that the Molar Weight (MW) of TYR is 137,18 g mol^{-1}, the molar concentration of TYR (c_{TYR}) can be computed as:

$$c_{TYR} = \frac{MW_{TYR}}{\rho_{TYR}} \tag{23}$$

Since in the spectrophotometer was analysed a solution of 1.5 mg in 1.5 mL, the volume of the solution to be considered is mL. Therefore the number of moles of TYR in mL of solution is:

$$n_{TYR} = c_{TYR} \cdot 1.5; \tag{24}$$

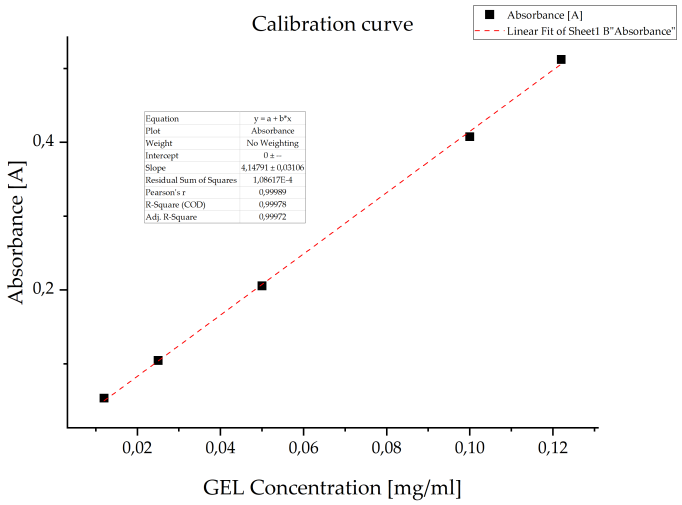

Figure 31: Calibration curve for tyramine concentration in a solution based on absorbance at 275 nm.

Then, we have to compute the numbers of COOH moles in the solution: according to the manufacturer's data, there are 0.0008 mol of COOH groups each gram of GEL. Therefore, in 1.5 mg of GEL the number of moles of COOH groups is:

$$n_{COOH} = m_{GEL} \cdot 0.0008 \cdot 1/1000 = 0.0000012 molmol \tag{25}$$

Since 1 molecule of TYR reacts with 1 molecule of COOH, the moles of COOH bound with TYR are the same as the moles of TYR. These moles are referred as *occupied moles* i order to differentiated them to the COOH moles that are not linked with TYR (*free moles*) Thus, the number of *free* COOH is equal to the number of initial COOH minus the number of COOH occupied.

$$n_{freeCOOH} = n_{COOH} - n_{occCOOH} \tag{26}$$

If you have 0.0000012 mol of *free* COOH then the 'freedom' of the COOH is 100% (you have nothing attached to it), therefore:

$$\%COOH_{free} = \frac{n_{freeCOOH}}{n_{COOH}} \cdot 100 \tag{27}$$

Therefore, the % of *occupied* COOH, in which the binding to TYR has occurred, is 100- $\%COOH_{free}$. This value gives the degree of styramine substitution.

$$degreeofsubstitution = 100 - \%COOH_{free} \tag{28}$$

These calculations were implemented in Matlab with the following code. In this way, the degree of substitution can be obtained simply by providing the absorbance spectrum as input.

- definition of *degreetyr* MATLAB function

Listing 1: Matlab code used for the calculation of the degree of substitution of tyramine

```
function [tyr_degree_sub,lambda_real,vec_275,std_275,abs
    _275] = degreetyr(name)
% This function requires as input an excel file with the
    absorbance values measured by the spectrophotometer and
    provides several outputs: the degree of tyramine
    substitution, the wavelength closest to 275 nm measured
    by the spectrophotometer and their standard deviation,
    the absorbance values measured at that wavelength.
```

- load data

```
data_stru=importdata(name);
data=data_stru.data;
lambda=data(:,1); % wavelength
temp=nan(length(lambda),3); % preallocating the matrix
temp(:,1)=data(:,2); %sample 1
temp(:,2)=data(:,4); %sample 2
temp(:,3)=data(:,6); %sample 3
```

- Calculation of the the closest wavelength to 275 nm measured by the spectrophotometer

```
abs_mean=mean(temp,2); %vector of absorbance mean values
val_abs=275; %nm , target value
residue=abs(lambda-val_abs); %  residues vector
[~,pos]=min(residue); % find the index of the minimum
    residue
vec_275=temp(pos,:);
std_275=std(vec_275);
lambda_real=lambda(pos); %nearest lambda to 275 nm on the
    excel file
abs_275=abs_mean(pos); %value of the mean absorbance at that
     lambda
```

- Calibration line

```
%% Calculation of the approximation line
 x=[0.0125, 0.025, 0.05, 0.1, 0.125]; %concentrations
 y=[0.05355, 0.1045, 0.20555, 0.40755, 0.5122]; %abs value
 [poly]=polyfit(x,y,1) %computes the angular coefficient and
      intercept of the least square line interpolating the
     data
 m=poly(1);
 q=poly(2);
```

- Calculation of tyramine concentration

```
%% Calculation of the degree of substitution
mol_cooh_100=0.08; % moles of COOH in 100 g of gel
mass_gelatine=1.5*10^-3; %grams
mol_cooh=mol_cooh_100*mass_gelatine/100; %Moles of COOH in
    1.5 mg of gel
% The concentration of Tyr using the calibration line is
% C_tyr=Abs-q/(m); % (Abs=m*(C_tyr))
C_tyr_mgml=abs_275/m; %mg/ml
PM_tyr=137.18; %g/mol
C_tyr_molml=C_tyr_mgml/(PM_tyr*1000); %mol/ml
```

- Calculation of tyramine degree based on free COOH moles

```
% Since in the spectrophotometer you prepare a solution of
    1.5 mg in 1.5 ml, you use a volume of 1.5 ml. Therefore
    the number of moles of Tyr in 1.5 ml is:
moles_tyr=C_tyr_molml*1.5;
% Since 1 molecule of Tyr reacts with 1 molecule of COOH,
    the moles of COOH occupied are the same as the moles of
    Tyr.
moles_cooh_occupied=moles_tyr;
% Thus, the number of free COOH is equal to the number of
    initial COOH minus the number of free NO COOH.
moles_cooh_free=mol_cooh-moles_cooh_occupied;
% If you have 0.0000012 mol of free COOH then the 'freedom'
    of the COOH is 100% (you have nothing attached to it),
    therefore:
perc_cooh_free=moles_cooh_free*100/mol_cooh;
%Therefore, the % of NO free COOH, i.e. in which the binding
     to Tyr has occurred, is 100-x
tyr_degree_sub=100-perc_cooh_free;
end
```

C

CALCULATIONS FOR HYDROGELS SYNTHESIS

The main objective of this appendix is to show the calculations done to calculate the proportions and mass of the different reactants in the synthesis of hydrogels. To perform the different experiments, has been utilized hydrogels of two different volumes: 200 µL and 550 µL. All the calculation refer to a single hydrogel.

C.1 HYDROGELS WITHOUT HEPARIN

C.1.1 *Pure hydrogels*

Table 21 shows the exact volumes of the regents used for pure GEL hydrogels. Table 22 refers to pure ELR hydrogels with VKV-N_3, while Table 23 to pure ELR hydrogels with HBD6-N_3.

C.1.2 *Intermediate blends*

The intermediate blends synthesized are:

- GEL/ELR 75/25
- GEL/ELR 50/50
- GEL/ELR 25/75

Table 25 shows the exact volumes of the regents used for GEL/ELR 75/25 hydrogels, Table 24 shows the exact volumes of the regents used for GEL/ELR 50/50 hydrogels and Table 26 shows the exact volumes of the regents used for GEL/ELR 25/75 hydrogels.

Table 21: Volume of reagents for pure GEL hydrogels

Reagents	Concentration	Volume fraction	Volume hydrogel	
			200 µL	550 µL
GEL	40 mg mL^{-1}	80%	160 µL	440 µL
HRP	12,5 mL^{-1}	10%	20 µL	55 µL
H_2O_2	20 mM	10%	20 µL	55 µL

Table 22: Volume of reagents for pure VKV-ELR hydrogels

Reagents	Concentration	Volume fraction	Volume hydrogel	
			200 µL	550 µL
VKV-N3	40 mg mL^{-1}	50%	100 µL	275 µL
VKV-CC	40 mg mL^{-1}	50%	100 µL	275 µL

Table 23: Volume of reagents for pure HBD6-ELR hydrogels

Reagents	Concentration	Volume fraction	Volume hydrogel	
			200 µL	550 µL
HBD6-N3	40 mg mL^{-1}	50%	100 µL	275 µL
VKV-CC	40 mg mL^{-1}	50%	100 µL	275 µL

Table 24: Volume of reagents for GEL-ELR 50/50 hydrogels

Reagents	Concentration	Volume fraction	Volume hydrogel	
			200 µL	550 µL
HBD6-N3	40 mg mL^{-1}	25%	50 µL	137,5 µL
HRP	12,5 mL^{-1}	5%	10 µL	27,5 µL
VKV-CC	40 mg mL^{-1}	25%	50 µL	137,5 µL
GEL	40 mg mL^{-1}	40%	80 µL	220 µL
H2O2	20 mM	5%	10 µL	27,5 µL

Table 25: Volume of reagents for GEL-TYR 75/25 hydrogels

Reagents	Concentration	Volume fraction	Volume	
			200 µL	**550 µL**
HBD6-N3	40 mg mL^{-1}	12,5%	25 µL	68,75 µL
HRP	12,5 mL^{-1}	7,5%	15 µL	41,25 µL
VKV-CC	40 mg mL^{-1}	12,5%	25 µL	68,75 µL
GEL	40 mg mL^{-1}	60,0%	120 µL	330 µL
H2O2	20 mM	10,0%	20	55 µL

Table 26: Volume of reagents for GEL-TYR 25/75 hydrogels

Reagents	Concentration	Volume fraction	Volume	
			200 µL	550 µL
HBD6-N3	40 mg mL^{-1}	37,5%	75 µL	206,25 µL
HRP	12,5 mL^{-1}	2,5%	5 µL	13,75 µL
VKV-CC	40 mg mL^{-1}	37,5%	75 µL	206,25 µL
GEL	40 mg mL^{-1}	20,0%	40 µL	110 µL
H2O2	20 mM	2,5%	5 µL	13,75 µL

C.2 HYDROGELS WITH HEPARIN

For the heparin release test, hydrogels with a volume of 200 µL were formed. However, as heparin also had to be included in the total volume, the volumes of the other reagents had to be adjusted accordingly. The heparin solution had a concentration of 20 mg mL^{-1} in DMEM. The final concentration of heparin in the hydrogels was set at 1mg mL^{-1}. Therefore, 0.2 mg of heparin should be present in a volume of 200 µL hydrogel. Thus, in order to obtain that mass of heparin from a heparin solution of 20 mg mL^{-1}, 10 µl of this solution must be added to HBD6-N_3 volume.

C.3 HYDROGELS WITH HGF

For the HGF release test, hydrogels with a volume of 50 µL were formed.

HGF AND HEPARIN As both heparin and HGF had to be included in the total hydrogel volume, the volumes of the other reagents had to be adjusted accordingly. The heparin solution had a concentration of 20 mg mL^{-1} in DMEM. The final concentration of heparin in the hydrogels was set at 0.1mg mL^{-1}. Therefore, 0.05 mg of heparin should be present in a volume of 50 µL. Thus, in order to obtain that mass of heparin from a heparin solution of 2.5 mg mL^{-1}, 2 µL of this solution must be added to HBD6-N_3 volume. The HGF solution had a concentration of 100 µg mL^{-1} in DMEM. The final concentration of HGF in the hydrogels was set at 10 µg mL^{-1}. Therefore, 0.5 µg of HGF should be present in a volume of 50 µL hydrogel. Thus, in order to obtain that mass of HGF from a heparin solution of 100 µg mL^{-1}, 5 µL of this solution must be added to HBD6-N_3 volume. Therefore, HBD6-N_3 volume was obtain by subtracting 7 µL to volume show in Table 24.

HGF As only HGF had to be included into the hydrogel, HBD6-N_3 volume was obtain by subtracting 5 µL to volume show in Table 24.

D

CALCULATIONS FOR HEPARIN RELEASE

The main objective of this appendix is to show the calculations performed to calculate the heparin release of hydrogels.

D.1 FLUORESCENT HEPARIN METHOD

By means of the spectrophotometer, we obtained the fluorescence excitation values of the supernatants referred to the 5 hydrogels analysed at the 6 different times indicated in Table 3, consequently measuring 30 different values. The calibration curve (Figure 14) showed the following relationship between the fluorescence F_{535} measured and heparin concentration:

$$F_{535} = 1131548.55 \cdot C_{Hep}[mg\,mL^{-1}] + 503 \tag{29}$$

Knowing that:

$$m_{Hep} = C_{Hep} \cdot V_{sol} \tag{30}$$

where V_{sol} is the volume of the supernatant (1 mL), it was possible to calculate the mass of heparin in the supernatant [$m_{hep}[mg]$] as:

$$m_{Hep} = \frac{(F_{535} - 503) \cdot V_{sol}}{1131548.55} \tag{31}$$

In our case, we worked with a supernatant volume of 1 mL, so the numerical value of the concentration was equal to the value of the mass of heparin released. Finally, once the values of the mass of heparin released at each time step ($m_{Hep}(t)$) were obtained, these values were meaned in order to obtain a mean value and standard deviation of heparin mass released at each of the six time frames measured. Thus, we added together these mean values to obtain the mean cumulative mass of heparin released.

$$m_{Hep}tot = \sum_{t=1}^{n} m_{Hep}(t) \tag{32}$$

To calculate the standard deviation of the cumulative mass of heparin released, we relied on the following error theory formula:

$$\sigma_f = \sqrt{\sum_{i=1}^{n} \sigma_i^2 \cdot \left(\frac{\partial f(x_i)}{\partial x_i}\right)^2} \tag{33}$$

Where $f(x_i)$ represent in our case $f = \sum_{i=1}^{n} x_i$

E

CALCULATIONS FOR HGF RELEASE

E.1 CALIBRATION LINE

To prepare the calibration line, the fluorescence of nine dilutions of labelled protein in PBS at a known concentration was measured three times. The concentration are shown in Table 27. Each sample was 100 µL so 350 µL of each dilution was prepared. The stock solution had a concentration of 100 $\mu g\,mL^{-1}$, so it was necessary to calculate the volume that had to be taken from this solution in order to obtain a initial concentration of 2 $\mu g\,mL^{-1}$. This calculation required knowing the total volume of the most concentrated solution, and to obtain this result, it was necessary to proceed backwards from the lowest concentration. In this way, once the desired volume was fixed, we could proceed to calculate the volume of dilutions at higher concentrations.

Table 27: HGF calibration line

C [$\mu g\,mL^{-1}$]	V tot [µL]	V sample [µL]	V_{PBS} [µL]	V_{prev} [µL]
0,015625	350	350-350=0	175	175
0,03125	525	525-350=175	263	263
0,0625	612	312-350=262	306	306
0,125	656	656-350=306	328	328
0,25	678	368-350=328	339	339
0,5	689	689-350=339	345	345
1	694	694-350=344	347	347
2	697	397-350=347	-	-

Thus, 697 µL of 2 $\mu g\,mL^{-1}$ solution of HGF-488 on PBS were required. As the stock solution had a concentration of 100 $\mu g\,mL^{-1}$, the volume that had to be taken from this was:

$$C_i \cdot V_i = C_f \cdot V_f \tag{34}$$

$$V_i = \frac{2[\mu g\,mL^{-1}] \cdot 697[\mu L]}{100[\mu g\,mL^{-1}]} = 14\mu L \tag{35}$$

Therefore, the initial solution was prepared with 14 µL of 100 [$\mu g\,mL^{-1}$] HGF-488 solution in PBS and 683 µL of PBS.

E.2 CALCULATION OF CUMULATIVE RELEASE

By means of the spectrophotometer, we obtained the fluorescence excitation values of the supernatants referred to the hydrogels analyzed at the 6 different times indicated in Table 3 and with three technical replicates for each supernatant. By means of the calibration curve showed on Section 3.8, was possible to obtain the HGF concentration into the supernatant. As for the interpolation was used a third degree polynomial, this calculation was done trough numerical methods with MATLAB. Finally, once the values of the mass of HGF released at each time step ($m_{Hep}(t)$) were obtained, these values were meaned in order to obtain a mean value and standard deviation of HGF mass released at each of the six time frames measured. Thus, we added together these mean values to obtain the mean cumulative mass of HGF released.

$$m_{HGF}tot = \sum_{t=1}^{n} m_{HGF}(t) \tag{36}$$

To calculate the standard deviation of the cumulative mass of HGF released, we relied on the following error theory formula:

$$\sigma_f = \sqrt{\sum_{i=1}^{n} \sigma_i^2 \cdot \left(\frac{\partial f(x_i)}{\partial x_i}\right)^2} \tag{37}$$

Where $f(x_i)$ represent in our case $f = \sum_{i=1}^{n} x_i$

BIBLIOGRAPHY

[1] Himanshu Kaul and Yiannis Ventikos. «On the Genealogy of Tissue Engineering and Regenerative Medicine.» en. In: *Tissue Engineering Part B: Reviews* 21.2 (Apr. 2015), pp. 203–217. ISSN: 1937-3368, 1937-3376. DOI: 10.1089/ten.teb.2014.0285. URL: https://www.liebertpub.com/doi/10.1089/ten.teb.2014.0285 (visited on 05/30/2022).

[2] Andreas G Nerlich, Albert Zink, Ulrike Szeimies, and Hjalmar G Hagedorn. «Ancient Egyptian prosthesis of the big toe.» en. In: *The Lancet* 356.9248 (Dec. 2000), pp. 2176–2179. ISSN: 01406736. DOI: 10.1016/S0140-6736(00)03507-8. URL: https://linkinghub.elsevier.com/retrieve/pii/S0140673600035078 (visited on 05/30/2022).

[3] Ali Khademhosseini and Robert Langer. «A decade of progress in tissue engineering.» en. In: *Nature Protocols* 11.10 (Oct. 2016), pp. 1775–1781. ISSN: 1754-2189, 1750-2799. DOI: 10.1038/nprot.2016.123. URL: https://www.nature.com/articles/nprot.2016.123 (visited on 05/02/2022).

[4] G. Androutsos, A. Diamantis, and L. Vladimiros. «The first leg transplant for the treatment of a cancer by Saints Cosmas and Damian.» eng. In: *Journal of B.U.ON.: official journal of the Balkan Union of Oncology* 13.2 (June 2008), pp. 297–304. ISSN: 1107-0625.

[5] Robert Langer, Joseph P. Vacanti, Charles A. Vacanti, Anthony Atala, Lisa E. Freed, and Gordana Vunjak-Novakovic. «Tissue Engineering: Biomedical Applications.» en. In: *Tissue Engineering* 1.2 (June 1995), pp. 151–161. ISSN: 1076-3279, 1557-8690. DOI: 10.1089/ten.1995.1.151. URL: https://www.liebertpub.com/doi/10.1089/ten.1995.1.151 (visited on 04/28/2022).

[6] Shinya Yamanaka. «Strategies and New Developments in the Generation of Patient-Specific Pluripotent Stem Cells.» en. In: *Cell Stem Cell* 1.1 (June 2007), pp. 39–49. ISSN: 19345909. DOI: 10.1016/j.stem.2007.05.012. URL: https://linkinghub.elsevier.com/retrieve/pii/S1934590907000185 (visited on 05/30/2022).

[7] Joseph A DiMasi, Ronald W Hansen, and Henry G Grabowski. «The price of innovation: new estimates of drug development costs.» en. In: *Journal of Health Economics* 22.2 (Mar. 2003), pp. 151–185. ISSN: 01676296. DOI: 10.1016/S0167-6296(02)00126-1. URL: https://linkinghub.elsevier.com/retrieve/pii/S0167629602001261 (visited on 05/30/2022).

[8] Colle Io. «Assessing Pharmaceutical Research and Development Costs.» en. In: (2018), p. 3.

[9] Jen-Yin Goh, Richard J. Weaver, Libby Dixon, Nicola J. Platt, and Ruth A. Roberts. «Development and use of in vitro alternatives to animal testing by the pharmaceutical industry 1980–2013.» en. In: *Toxicology Research* 4.5 (2015), pp. 1297–1307. ISSN: 2045-452X, 2045-4538. DOI: 10.1039/C5TX00123D. URL: https://academic.oup.com/toxres/article/4/5/1297-1307/5573503 (visited on 05/30/2022).

[10] Susan Standring, ed. *Gray's anatomy: the anatomical basis of clinical practice*. en. Forty-first edition. New York: Elsevier Limited, 2016. ISBN: 978-0-7020-5230-9 978-0-7020-6306-0.

[11] Sherif R.Z. Abdel-Misih and Mark Bloomston. «Liver Anatomy.» en. In: *Surgical Clinics of North America* 90.4 (Aug. 2010), pp. 643–653. ISSN: 00396109. DOI: 10.1016/j.suc.2010.04.017. URL: https://linkinghub.elsevier.com/retrieve/pii/S0039610910000526 (visited on 05/21/2022).

[12] «7 - UPPER ABDOMINAL VISCERA.» In: *Ultrasonic Sectional Anatomy*. Ed. by Patricia Morley, Gabriel Donald, and Roger Sanders. Elsevier, 1983, pp. 63–98. ISBN: 978-0-443-01690-5. DOI: https://doi.org/10.1016/B978-0-443-01690-5.50015-8. URL: https://www.sciencedirect.com/science/article/pii/B9780443016905500158.

[13] Ajit Dash, Walker Inman, Keith Hoffmaster, Samantha Sevidal, Joan Kelly, R Scott Obach, Linda G Griffith, and Steven R Tannenbaum. «Liver tissue engineering in the evaluation of drug safety.» en. In: *Expert Opinion on Drug Metabolism & Toxicology* 5.10 (Oct. 2009), pp. 1159–1174. ISSN: 1742-5255, 1744-7607. DOI: 10.1517/17425250903160664. URL: http://www.tandfonline.com/doi/full/10.1517/17425250903160664 (visited on 04/30/2022).

[14] Hui Yun Zhou, Yan Ping Zhang, Wei Fen Zhang, and Xi Guang Chen. «Biocompatibility and characteristics of injectable chitosan-based thermosensitive hydrogel for drug delivery.» en. In: *Carbohydrate Polymers* 83.4 (Feb. 2011), pp. 1643–1651. ISSN: 01448617. DOI: 10.1016/j.carbpol.2010.10.022. URL: https://linkinghub.elsevier.com/retrieve/pii/S0144861710008283 (visited on 06/08/2022).

[15] George K. Michalopoulos and Bharat Bhushan. «Liver regeneration: biological and pathological mechanisms and implications.» en. In: *Nature Reviews Gastroenterology & Hepatology* 18.1 (Jan. 2021), pp. 40–55. ISSN: 1759-5045, 1759-5053. DOI: 10.1038/s41575-020-0342-4. URL: https://www.nature.com/articles/s41575-020-0342-4 (visited on 05/21/2022).

[16] Lixin Ke, Cuncun Lu, Rui Shen, Tingting Lu, Bin Ma, and Yunpeng Hua. «Knowledge Mapping of Drug-Induced Liver Injury: A Scientometric Investigation (2010–2019).» en. In: *Frontiers in Pharmacology* 11 (June 2020), p. 842. ISSN: 1663-9812. DOI: 10.3389/fphar.2020.00842. URL: https://www.frontiersin.org/article/10.3389/fphar.2020.00842/full (visited on 05/13/2022).

[17] Raul J. Andrade et al. «Drug-induced liver injury.» eng. In: *Nature Reviews. Disease Primers* 5.1 (Aug. 2019), p. 58. ISSN: 2056-676X. DOI: 10.1038/s41572-019-0105-0.

[18] Gerd A Kullak-Ublick, Raul J Andrade, Michael Merz, Peter End, Andreas Benesic, Alexander L Gerbes, and Guruprasad P Aithal. «Drug-induced liver injury: recent advances in diagnosis and risk assessment.» en. In: *Gut* 66.6 (June 2017), pp. 1154–1164. ISSN: 0017-5749, 1468-3288. DOI: 10.1136/gutjnl-2016-313369. URL: https://gut.bmj.com/lookup/doi/10.1136/gutjnl-2016-313369 (visited on 05/13/2022).

[19] Louis Leung, Amit S. Kalgutkar, and R. Scott Obach. «Metabolic activation in drug-induced liver injury.» en. In: *Drug Metabolism Reviews* 44.1 (Feb. 2012), pp. 18–33. ISSN: 0360-2532, 1097-9883. DOI: 10.3109/03602532.2011.605791. URL: http://www.tandfonline.com/doi/full/10.3109/03602532.2011.605791 (visited on 05/29/2022).

[20] Jack Uetrecht. «Mechanistic Studies of Idiosyncratic DILI: Clinical Implications.» en. In: *Frontiers in Pharmacology* 10 (July 2019), p. 837. ISSN: 1663-9812. DOI: 10.3389/fphar.2019.00837. URL: https://www.frontiersin.org/article/10.3389/fphar.2019.00837/full (visited on 05/13/2022).

[21] B. Kevin Park et al. «Managing the challenge of chemically reactive metabolites in drug development.» en. In: *Nature Reviews Drug Discovery* 10.4 (Apr. 2011), pp. 292–306. ISSN: 1474-1776, 1474-1784. DOI: 10.1038/nrd3408. URL: http://www.nature.com/articles/nrd3408 (visited on 05/29/2022).

[22] Laia Tolosa, Nuria Jiménez, Gabriela Pérez, José V. Castell, M. José Gómez-Lechón, and M. Teresa Donato. «Customised in vitro model to detect human metabolism-dependent idiosyncratic drug-induced liver injury.» en. In: *Archives of Toxicology* 92.1 (Jan. 2018), pp. 383–399. ISSN: 0340-5761, 1432-0738. DOI: 10.1007/s00204-017-2036-4. URL: http://link.springer.com/10.1007/s00204-017-2036-4 (visited on 05/13/2022).

[23] B. S. MohanKumar, G. Priyanka, S. Rajalakshmi, Rakesh Sankar, Taj Sabreen, and Jayasree Ravindran. «Hydrogels: potential aid in tissue engineering—a review.» en. In: *Polymer Bulletin* (Sept. 2021). ISSN: 0170-0839, 1436-2449. DOI: 10.1007/s00289-021-

03864-x. URL: https://link.springer.com/10.1007/s00289-021-03864-x (visited on 05/28/2022).

[24] Seblewongel Petros, Tamrat Tesfaye, and Million Ayele. «A Review on Gelatin Based Hydrogels for Medical Textile Applications.» en. In: *Journal of Engineering* 2020 (Dec. 2020). Ed. by Huining Xiao, pp. 1–12. ISSN: 2314-4912, 2314-4904. DOI: 10.1155/2020/8866582. URL: https://www.hindawi.com/journals/je/2020/8866582/ (visited on 05/28/2022).

[25] Jin Hyun Lee. «Injectable hydrogels delivering therapeutic agents for disease treatment and tissue engineering.» en. In: *Biomaterials Research* 22.1 (Dec. 2018), p. 27. ISSN: 2055-7124. DOI: 10.1186/s40824-018-0138-6. URL: https://biomaterialsres.biomedcentral.com/articles/10.1186/s40824-018-0138-6 (visited on 05/28/2022).

[26] Patricio Godoy et al. «Recent advances in 2D and 3D in vitro systems using primary hepatocytes, alternative hepatocyte sources and non-parenchymal liver cells and their use in investigating mechanisms of hepatotoxicity, cell signaling and ADME.» en. In: *Archives of Toxicology* 87.8 (Aug. 2013), pp. 1315–1530. ISSN: 0340-5761, 1432-0738. DOI: 10.1007/s00204-013-1078-5. URL: http://link.springer.com/10.1007/s00204-013-1078-5 (visited on 05/13/2022).

[27] J. Elisseeff, K. Anseth, D. Sims, W. McIntosh, M. Randolph, and R. Langer. «Transdermal photopolymerization for minimally invasive implantation.» In: *Proceedings of the National Academy of Sciences of the United States of America* 96.6 (Mar. 1999), pp. 3104–3107. ISSN: 0027-8424. URL: https://www.ncbi.nlm.nih.gov/pmc/articles/PMC15902/ (visited on 06/21/2022).

[28] Enas M. Ahmed. «Hydrogel: Preparation, characterization, and applications: A review.» en. In: *Journal of Advanced Research* 6.2 (Mar. 2015), pp. 105–121. ISSN: 20901232. DOI: 10.1016/j.jare.2013.07.006. URL: https://linkinghub.elsevier.com/retrieve/pii/S2090123213000969 (visited on 05/02/2022).

[29] Keming Xu, Fan Lee, Shu Jun Gao, Joo Eun Chung, Hirohisa Yano, and Motoichi Kurisawa. «Injectable hyaluronic acid-tyramine hydrogels incorporating interferon-2a for liver cancer therapy.» en. In: *Journal of Controlled Release* 166.3 (Mar. 2013), pp. 203–210. ISSN: 01683659. DOI: 10.1016/j.jconrel.2013.01.008. URL: https://linkinghub.elsevier.com/retrieve/pii/S0168365913000254 (visited on 06/08/2022).

[30] Esther Sanmartín-Masiá, Sara Poveda-Reyes, and Gloria Gallego Ferrer. «Extracellular matrix-inspired gelatin/hyaluronic acid injectable hydrogels.» en. In: (), p. 35.

[31] Resmi Rajalekshmi, Anusree Kaladevi Shaji, Roy Joseph, and Anugya Bhatt. «Scaffold for liver tissue engineering: Exploring the potential of fibrin incorporated alginate dialdehyde–gelatin hydrogel.» en. In: *International Journal of Biological Macromolecules* 166 (Jan. 2021), pp. 999–1008. ISSN: 01418130. DOI: 10.1016/j.ijbiomac.2020.10.256. URL: https://linkinghub.elsevier.com/retrieve/pii/S0141813020349084 (visited on 04/30/2022).

[32] S. Van Vlierberghe, P. Dubruel, and E. Schacht. «Biopolymer-Based Hydrogels As Scaffolds for Tissue Engineering Applications: A Review.» en. In: *Biomacromolecules* 12.5 (May 2011), pp. 1387–1408. ISSN: 1525-7797, 1526-4602. DOI: 10.1021/bm200083n. URL: https://pubs.acs.org/doi/10.1021/bm200083n (visited on 05/02/2022).

[33] Gang Yang, Zhenghua Xiao, Haiyan Long, Kunlong Ma, Junpeng Zhang, Xiaomei Ren, and Jiang Zhang. «Assessment of the characteristics and biocompatibility of gelatin sponge scaffolds prepared by various crosslinking methods.» en. In: *Scientific Reports* 8.1 (Dec. 2018), p. 1616. ISSN: 2045-2322. DOI: 10.1038/s41598-018-20006-y. URL: http://www.nature.com/articles/s41598-018-20006-y (visited on 05/28/2022).

[34] Kim A. Luetchford, Julian B. Chaudhuri, and Paul A. De Bank. «Silk fibroin/gelatin microcarriers as scaffolds for bone tissue engineering.» en. In: *Materials Science and Engineering: C* 106 (Jan. 2020), p. 110116. ISSN: 09284931. DOI: 10.1016/j.msec.2019.110116. URL: https://linkinghub.elsevier.com/retrieve/pii/S0928493118328911 (visited on 06/08/2022).

[35] Erkki Ruoslahti. «RGD AND OTHER RECOGNITION SEQUENCES FOR INTEGRINS.» en. In: *Annual Review of Cell and Developmental Biology* 12.1 (Nov. 1996), pp. 697–715. ISSN: 1081-0706, 1530-8995. DOI: 10.1146/annurev.cellbio.12.1.697. URL: https://www.annualreviews.org/doi/10.1146/annurev.cellbio.12.1.697 (visited on 05/28/2022).

[36] Michael D. Pierschbacher and Erkki Ruoslahti. «Cell attachment activity of fibronectin can be duplicated by small synthetic fragments of the molecule.» en. In: *Nature* 309.5963 (May 1984), pp. 30–33. ISSN: 0028-0836, 1476-4687. DOI: 10.1038/309030a0. URL: http://www.nature.com/articles/309030a0 (visited on 05/28/2022).

[37] Natalia Davidenko, Carlos F. Schuster, Daniel V. Bax, Richard W. Farndale, Samir Hamaia, Serena M. Best, and Ruth E. Cameron. «Evaluation of cell binding to collagen and gelatin: a study of theeffect of 2D and 3D architecture and surface chemistry.» en. In: *Journal of Materials Science: Materials in Medicine* 27.10 (Oct. 2016), p. 148. ISSN: 0957-4530, 1573-4838. DOI: 10.1007/s10856-

016-5763-9. URL: http://link.springer.com/10.1007/s10856-016-5763-9 (visited on 05/25/2022).

[38] Makoto Ozeki and Yasuhiko Tabata. «Affinity evaluation of gelatin for hepatocyte growth factor of different types to design the release carrier.» en. In: *Journal of Biomaterials Science, Polymer Edition* 17.1-2 (Jan. 2006), pp. 139–150. ISSN: 0920-5063, 1568-5624. DOI: 10.1163/156856206774879027. URL: https://www.tandfonline.com/doi/full/10.1163/156856206774879027 (visited on 04/30/2022).

[39] D.G. Hoare and D.E. Koshland. «A Method for the Quantitative Modification and Estimation of Carboxylic Acid Groups in Proteins.» en. In: *Journal of Biological Chemistry* 242.10 (May 1967), pp. 2447–2453. ISSN: 00219258. DOI: 10.1016/S0021-9258(18)95981-8. URL: https://linkinghub.elsevier.com/retrieve/pii/S0021925818959818 (visited on 05/28/2022).

[40] Shinji Sakai, Keisuke Hirose, Kenichi Taguchi, Yuko Ogushi, and Koei Kawakami. «An injectable, in situ enzymatically gellable, gelatin derivative for drug delivery and tissue engineering.» en. In: *Biomaterials* 30.20 (July 2009), pp. 3371–3377. ISSN: 01429612. DOI: 10.1016/j.biomaterials.2009.03.030. URL: https://linkinghub.elsevier.com/retrieve/pii/S0142961209003007 (visited on 05/21/2022).

[41] Ursula R. Rodgers and Anthony S. Weiss. «Cellular interactions with elastin.» en. In: *Pathologie Biologie* 53.7 (Sept. 2005), pp. 390–398. ISSN: 03698114. DOI: 10.1016/j.patbio.2004.12.022. URL: https://linkinghub.elsevier.com/retrieve/pii/S0369811404003116 (visited on 05/04/2022).

[42] J. Carlos Rodríguez-Cabello, Laura Martín, Matilde Alonso, F. Javier Arias, and Ana M. Testera. «"Recombinamers" as advanced materials for the post-oil age.» en. In: *Polymer* 50.22 (Oct. 2009), pp. 5159–5169. ISSN: 00323861. DOI: 10.1016/j.polymer.2009.08.032. URL: https://linkinghub.elsevier.com/retrieve/pii/S0032386109007290 (visited on 05/03/2022).

[43] Ming Miao, Catherine M. Bellingham, Richard J. Stahl, Eva E. Sitarz, Christopher J. Lane, and Fred W. Keeley. «Sequence and Structure Determinants for the Self-aggregation of Recombinant Polypeptides Modeled after Human Elastin.» en. In: *Journal of Biological Chemistry* 278.49 (Dec. 2003), pp. 48553–48562. ISSN: 00219258. DOI: 10.1074/jbc.M308465200. URL: https://linkinghub.elsevier.com/retrieve/pii/S0021925820756164 (visited on 05/04/2022).

[44] Alessandra Girotti, Alicia Fernández-Colino, Isabel M. López, José C. Rodríguez-Cabello, and Francisco J. Arias. «Elastin-like recombinamers: Biosynthetic strategies and biotechnological applications.» en. In: *Biotechnology Journal* 6.10 (2011), pp. 1174–

1186. ISSN: 1860-7314. DOI: 10.1002/biot.201100116. URL: https://onlinelibrary.wiley.com/doi/abs/10.1002/biot.201100116 (visited on 05/03/2022).

[45] Israel González de Torre, Mercedes Santos, Luis Quintanilla, Ana Testera, Matilde Alonso, and José Carlos Rodríguez Cabello. «Elastin-like recombinamer catalyst-free click gels: Characterization of poroelastic and intrinsic viscoelastic properties.» en. In: *Acta Biomaterialia* 10.6 (June 2014), pp. 2495–2505. ISSN: 17427061. DOI: 10.1016/j.actbio.2014.02.006. URL: https://linkinghub.elsevier.com/retrieve/pii/S1742706114000580 (visited on 05/01/2022).

[46] Jeremy M. Baskin and Carolyn R. Bertozzi. «Bioorthogonal Click Chemistry: Covalent Labeling in Living Systems.» en. In: *QSAR & Combinatorial Science* 26.11-12 (Dec. 2007), pp. 1211–1219. ISSN: 1611020X, 16110218. DOI: 10.1002/qsar.200740086. URL: https://onlinelibrary.wiley.com/doi/10.1002/qsar.200740086 (visited on 05/04/2022).

[47] Hartmuth C. Kolb, M. G. Finn, and K. Barry Sharpless. «Click Chemistry: Diverse Chemical Function from a Few Good Reactions.» en. In: *Angewandte Chemie International Edition* 40.11 (June 2001), pp. 2004–2021. ISSN: 1433-7851, 1521-3773. DOI: 10.1002/1521-3773(20010601)40:11<2004::AID-ANIE2004>3.0.CO;2-5. URL: https://onlinelibrary.wiley.com/doi/10.1002/1521-3773(20010601)40:11<2004::AID-ANIE2004>3.0.CO;2-5 (visited on 05/31/2022).

[48] R Huisgen. «Proceedings of the Chemical Society. October 1961.» In: *Proc. Chem. Soc.* October (1961). Publisher: The Royal Society of Chemistry, pp. 357–396. DOI: 10.1039/PS9610000357. URL: http://dx.doi.org/10.1039/PS9610000357.

[49] Dennis Svatunek, Gottfried Eilenberger, Christoph Denk, Daniel Lumpi, Christian Hametner, Günter Allmaier, and Hannes Mikula. «Live Monitoring of Strain-Promoted Azide Alkyne Cycloadditions in Complex Reaction Environments by Inline ATR-IR Spectroscopy.» en. In: 26.44 (2020), pp. 9851–9854. ISSN: 1521-3765. DOI: 10.1002/chem.201905478. URL: https://onlinelibrary.wiley.com/doi/abs/10.1002/chem.201905478 (visited on 05/31/2022).

[50] Nicholas J. Agard, Jennifer A. Prescher, and Carolyn R. Bertozzi. «A Strain-Promoted [3 + 2] Azide-Alkyne Cycloaddition for Covalent Modification of Biomolecules in Living Systems.» en. In: *Journal of the American Chemical Society* 126.46 (Nov. 2004), pp. 15046–15047. ISSN: 0002-7863, 1520-5126. DOI: 10.1021/ja044996f. URL: https://pubs.acs.org/doi/10.1021/ja044996f (visited on 05/31/2022).

[51] Robert Lanza, ed. *Principles of tissue engineering*. en. Waltham: Elsevier, 2020. ISBN: 978-0-12-818422-6.

[52] Manuel Salmerón-Sánchez and Matthew J. Dalby. «Synergistic growth factor microenvironments.» en. In: *Chemical Communications* 52.91 (2016), pp. 13327–13336. ISSN: 1359-7345, 1364-548X. DOI: 10.1039/C6CC06888J. URL: http://xlink.rsc.org/?DOI=C6CC06888J (visited on 05/21/2022).

[53] Mikaël M. Martino et al. «Growth Factors Engineered for Super-Affinity to the Extracellular Matrix Enhance Tissue Healing.» en. In: *Science* 343.6173 (Feb. 2014), pp. 885–888. ISSN: 0036-8075, 1095-9203. DOI: 10.1126/science.1247663. URL: https://www.science.org/doi/10.1126/science.1247663 (visited on 06/08/2022).

[54] Kangwon Lee, Eduardo A. Silva, and David J. Mooney. «Growth factor delivery-based tissue engineering: general approaches and a review of recent developments.» en. In: *Journal of The Royal Society Interface* 8.55 (Feb. 2011), pp. 153–170. ISSN: 1742-5689, 1742-5662. DOI: 10.1098/rsif.2010.0223. URL: https://royalsocietypublishing.org/doi/10.1098/rsif.2010.0223 (visited on 06/08/2022).

[55] Toshikazu Nakamura, Tsutomu Nishizawa, Mitchio Hagiya, Tatsuya Seki, Manabu Shimonishi, Atsushi Sugimura, Kosuke Tashiro, and Shin Shimizu. «Molecular cloning and expression of human hepatocyte growth factor.» en. In: *Nature* 342.6248 (Nov. 1989), pp. 440–443. ISSN: 0028-0836, 1476-4687. DOI: 10.1038/342440a0. URL: http://www.nature.com/articles/342440a0 (visited on 05/28/2022).

[56] Takashi Kato. «Biological roles of hepatocyte growth factor-Met signaling from genetically modified animals (Review).» en. In: *Biomedical Reports* (Oct. 2017). ISSN: 2049-9434, 2049-9442. DOI: 10.3892/br.2017.1001. URL: http://www.spandidos-publications.com/10.3892/br.2017.1001 (visited on 06/18/2022).

[57] *HGF hepatocyte growth factor [Homo sapiens (human)] - Gene - NCBI*. URL: https://www.ncbi.nlm.nih.gov/gene/3082 (visited on 06/18/2022).

[58] Esther Sanmartín-Masiá, Sara Poveda-Reyes, and Gloria Gallego Ferrer. «Extracellular matrix–inspired gelatin/hyaluronic acid injectable hydrogels.» In: *International Journal of Polymeric Materials and Polymeric Biomaterials* 66.6 (2017), pp. 280–288. DOI: 10.1080/00914037.2016.1201828. eprint: https://doi.org/10.1080/00914037.2016.1201828. URL: https://doi.org/10.1080/00914037.2016.1201828.

[59] Issa Katime and Eduardo Mendizábal. «Swelling Properties of New Hydrogels Based on the Dimethyl Amino Ethyl Acrylate Methyl Chloride Quaternary Salt with Acrylic Acid and 2-Methylene Butane-1,4-Dioic Acid Monomers in Aqueous Solutions.» en. In: *Materials Sciences and Applications* 01.03 (2010), pp. 162–167. ISSN: 2153-117X, 2153-1188. DOI: 10.4236/msa.2010.13026. URL: http://www.scirp.org/journal/doi.aspx?DOI=10.4236/msa.2010.13026 (visited on 03/27/2022).

[60] *Microscopía electrónica de barrido de emisión de campo : Electron Microscopy Service : UPV*. URL: http://www.upv.es/entidades/SME/info/859071normali.html (visited on 06/09/2022).

[61] Mehmet Ayyildiz, Ranan Gulhan Aktas, and Cagatay Basdogan. «Effect of solution and post-mortem time on mechanical and histological properties of liver during cold preservation.» en. In: *Biorheology* 51.1 (2014), pp. 47–70. ISSN: 0006355X. DOI: 10.3233/BIR-14007. URL: https://www.medra.org/servlet/aliasResolver?alias=iospress&doi=10.3233/BIR-14007 (visited on 03/26/2022).

[62] P K Smith and A K Mallia. «Calorimetric Method for the Assay of Heparin Content in Immobilized Heparin Preparations.» en. In: (), p. 8.

[63] *The 3Rs | NC3Rs*. URL: https://nc3rs.org.uk/who-we-are/3rs (visited on 06/08/2022).

[64] Sara Poveda-Reyes, Vladimira Moulisova, Esther Sanmartín-Masiá, Luis Quintanilla-Sierra, Manuel Salmerón-Sánchez, and Gloria Gallego Ferrer. «Gelatin—Hyaluronic Acid Hydrogels with Tuned Stiffness to Counterbalance Cellular Forces and Promote Cell Differentiation.» In: *Macromolecular Bioscience* 16.9 (2016). _eprint: https://onlinelibrary.wiley.com/doi/pdf/10.1002/mabi.201500469, pp. 1311–1324. ISSN: 1616-5195. DOI: 10.1002/mabi.201500469. URL: https://onlinelibrary.wiley.com/doi/abs/10.1002/mabi.201500469 (visited on 05/22/2022).

[65] Vladimíra Moulisová, Sara Poveda-Reyes, Esther Sanmartín-Masiá, Luis Quintanilla-Sierra, Manuel Salmerón-Sánchez, and Gloria Gallego Ferrer. «Hybrid Protein–Glycosaminoglycan Hydrogels Promote Chondrogenic Stem Cell Differentiation.» en. In: *ACS Omega* 2.11 (Nov. 2017), pp. 7609–7620. ISSN: 2470-1343, 2470-1343. DOI: 10.1021/acsomega.7b01303. URL: https://pubs.acs.org/doi/10.1021/acsomega.7b01303 (visited on 06/09/2022).

[66] Penelope C. Georges, Jia-Ji Hui, Zoltan Gombos, Margaret E. McCormick, Andrew Y. Wang, Masayuki Uemura, Rosemarie Mick, Paul A. Janmey, Emma E. Furth, and Rebecca G. Wells. «Increased stiffness of the rat liver precedes matrix deposition: implications for fibrosis.» en. In: *American Journal of Physiology-Gastrointestinal and Liver Physiology* 293.6 (Dec. 2007), G1147–

G1154. ISSN: 0193-1857, 1522-1547. DOI: 10.1152/ajpgi.00032.2007. URL: https://www.physiology.org/doi/10.1152/ajpgi.00032.2007 (visited on 06/09/2022).

[67] Lukas Gritsch, Federico L. Motta, Nicola Contessi Negrini, L'Hocine Yahia, and Silvia Farè. «Crosslinked gelatin hydrogels as carriers for controlled heparin release.» en. In: *Materials Letters* 228 (Oct. 2018), pp. 375–378. ISSN: 0167577X. DOI: 10.1016/j.matlet.2018.06.047. URL: https://linkinghub.elsevier.com/retrieve/pii/S0167577X18309522 (visited on 03/26/2022).

[68] Tom Pollak, Patrick Rooney, and Mark Hager. «Understanding Management and General Expenses in Nonprofits.» In: Nov. 2001.